Received: 30 July 2021 | Revised: 30 December 2021 | Accepted: 3 January 2022

DOI: 10.1002/cne.25297

RESEARCH ARTICLE

JCN RESEARCH IN SYSTEMS NEUROSCIENCE THE JOURNAL OF COMPARATIVE NEUROLOGY WILEY

Distribution of neurogranin-like immunoreactivity in the brain and sensory organs of the adult zebrafish

Anabel Alba-González[1,2] | Mónica Folgueira[1,2] | Antonio Castro[1,2] | Ramón Anadón[3] | Julián Yáñez[1,2]

[1] Department of Biology, Faculty of Sciences, University of A Coruña, A Coruña, Spain

[2] Centro de Investigaciones Científicas Avanzadas (CICA), University of A Coruña, A Coruña, Spain

[3] Department of Functional Biology, Faculty of Biology, University of Santiago de Compostela, Santiago de Compostela, Spain

Correspondence
Mónica Folgueira and Julián Yáñez, Department of Biology, Faculty of Sciences. University of A Coruña. Campus da Zapateira. 15008 A Coruña, Spain.
Email: m.folgueira@udc.es; julian.yanez@udc.es

Funding information
Predoctoral Fellowship from Xunta de Galicia, Grant/Award Number: ED481A-2019/003

[Correction added on 25 May 2022, after first online publication: The copyright line was changed.]

Abstract

We studied the expression of neurogranin in the brain and some sensory organs (barbel taste buds, olfactory organs, and retina) of adult zebrafish. Database analysis shows zebrafish has two paralog neurogranin genes (*nrgna* and *nrgnb*) that translate into three peptides with a conserved IQ domain, as in mammals. Western blots of zebrafish brain extracts using an anti-neurogranin antiserum revealed three separate bands, confirming the presence of three neurogranin peptides. Immunohistochemistry shows neurogranin-like expression in the brain and sensory organs (taste buds, neuromasts and olfactory epithelium), not being able to discern its three different peptides. In the retina, the most conspicuous positive cells were bipolar neurons. In the brain, immunopositive neurons were observed in all major regions (pallium, subpallium, preoptic area, hypothalamus, diencephalon, mesencephalon and rhombencephalon, including the cerebellum), a more extended distribution than in mammals. Interestingly, dendrites, cell bodies and axon terminals of some neurons were immunopositive, thus zebrafish neurogranins may play presynaptic and postsynaptic roles. Most positive neurons were found in primary sensory centers (viscerosensory column and medial octavolateral nucleus) and integrative centers (pallium, subpallium, optic tectum and cerebellum), which have complex synaptic circuitry. However, we also observed expression in areas not related to sensory or integrative functions, such

Abbreviations: A, anterior thalamic nucleus; APN, accessory pretectal nucleus; *ca*, anterior commissure; CC, cerebellar crest; Ccb, cerebellar corpus; *cg*, gustatory commissure; CiL, central nucleus of the hypothalamic lobe; CON, caudal octavolateral nucleus; CP, central posterior thalamic nucleus; *cven*, rhombencephalic ventral commissure; D, dorsal telencephalic area (pallium); Dc, central zone of D; Dd, dorsal zone of D; DiL, diffuse nucleus of the hypothalamic lobe; Dl, lateral zone of D; Dlv, ventral part of Dl; Dm, medial zone of D; Dp, posterior zone of D; DP, dorsal posterior thalamic nuclei; *dV*, descending trigeminal root; EG, eminentia granularis; *fr*, fasciculus retroflexus; gc, central gray; GC, retinal ganglion cell layer; GCL, granular cell layer; GL, glomerular layer; Hb, habenulae; Hc, caudal hypothalamic nucleus; Hd, dorsal nucleus of the periventricular hypothalamus; Hv, ventral nucleus of periventricular hypothalamus; IL, inferior lobe / hypothalamic lobe; INL, retinal inner nuclear layer; IO, inferior olive; Ip, interpeduncular nucleus; IPL, retinal inner plexiform layer; IRF, intermediate reticular formation; *lfb*, lateral forebrain bundle; LIX, glossopharyngeal lobe; *ll*, lateral lemniscus; LVII, facial lobe; LX, vagal lobe; M, Mauthner cell; Ma, Mauthner axon; MB, mammillary body; *mfb*, medial forebrain bundle; MFN, medial funicular nucleus; *mlf*, medial longitudinal fascicle; MON, medial octavolateral nucleus; NAT, anterior tuberal nucleus; nC, commissural nucleus of Cajal; NI, nucleus isthmi; nIII, oculomotor nucleus; NLV, lateral valvular nucleus; Nm, neuromast; NMLF, nucleus of the medial longitudinal fascicle; nV, trigeminal nerve; OB, olfactory bulb; OLM, retinal outer limiting membrane; OPL, retinal outer plexiform layer; OSL, photoreceptor outer segment layer; OT, optic tectum; *ot*, optic tract; PC, layer of outer and inner segments of photoreceptor cells; PGl, lateral preglomerular nucleus; PGm, medial preglomerular nucleus; PO, posterior pretectal nucleus; Ppa, parvocellular preoptic nucleus; Ppm, magnocellular preoptic nucleus; PSm, magnocellular superficial pretectal nucleus; PSp, parvocellular superficial pretectal nucleus; Pth, prethalamus; PTN, posterior tuberal nucleus; Pvo, paraventricular organ; Q, optic chiasm; rIII, oculomotor nerve root; RL, nucleus rostrolateralis; SAC, stratum album centrale; SFGS, stratum fibrosum et griseum superficiale; SGC, stratum griseum centrale; *sgt*, secondary gustatory tract; SGVN, secondary gustatory/visceral nucleus; SM, stratum marginale; SO, stratum opticum; SPV, stratum periventriculare; SRF, superior reticular formation; STN, sensory trigeminal nucleus; *sy*, sulcus ypsiloniformis; *tbc*, tectobulbaris cruciatus tract; *tbr*, tectobulbaris rectus tract; TGN, tertiary gustatory nucleus (of Yáñez et al., 2017); Th, thalamus; *tip*, isthmo-pretectal tract; TLa, torus lateralis; TLo, torus longitudinalis; *tob*, torobulbar tract; TPp, periventricular nucleus of the posterior tubercle; TS, torus semicircularis; V, ventral telencephalic area; Val, lateral division of the cerebellar valvula; Vam, medial division of the cerebellar valvula; Vc, central nucleus of V; Vcb, cerebellar valvula; Vd, dorsal nucleus of V; VIII, octaval nerve; Vl, lateral nucleus of V; Vm, motor root of the trigeminal nerve; Vs, supracommissural nucleus of V; Vv, ventral nucleus of V; X, vagal nerve; Xm, vagal motor nucleus

as in cerebrospinal fluid-contacting cells associated with the hypothalamic recesses, which exhibited high neurogranin-like immunoreactivity. Together, these results reveal important differences with the patterns reported in mammals, suggesting divergent evolution from the common ancestor.

KEYWORDS
Danio rerio, neurogranin, protein kinase C, RC3, teleost, zebrafish

1 | INTRODUCTION

The neuronal protein p17/RC3/neurogranin was initially purified and sequenced from bovine brain extracts (p17; Baudier et al., 1989, 1991) and, almost in parallel, identified based on the analysis of cDNA clones that showed differential expression between rat forebrain and cerebellum (RC3; Watson et al., 1990). Shortly after, Deloulme et al. (1991) showed that p17 and RC3 were the same protein, named neurogranin (Nrgn). This 78 amino acids peptide contains a consensus IQ-motif that has at least a binding domain for calmodulin (CaM) (Baudier et al., 1989, 1991; Deloulme et al., 1991; Prichard et al., 1999) and a serine site for protein kinase C (PKC) phosphorylation (Baudier et al., 1991). The distribution of neurogranin in the rodent forebrain has been shown based on in situ hybridization and immunohistochemistry, in particular, in neurons of the cortex and hippocampus, striatum, amygdala, subthalamus, and hypothalamus, with high expression in postsynaptic structures (dendrites, somas) (Represa et al., 1990; Watson et al., 1990, 1992). Various studies have revealed that nonphosphorylated neurogranin appears to regulate neuronal activity via postsynaptic binding to the Ca^{2+} free form of CaM, modulating phosphorylation of proteins by Ca^{2+}/CaM-dependent PKCs and resulting in synaptic plasticity (Díez-Guerra, 2010; Slemmon et al., 2000; Zhong & Gerges, 2012). A well-characterized effect is long-term potentiation (LTP) induction, which requires the activation of NMDA receptors and an increase in the Ca^{2+} concentration within dendritic spines (Zhong & Gerges, 2012). Neurogranin appears involved in higher neural processing such as learning, adaptation and memory formation (Zhong et al., 2015). Several studies also suggested a potential relation of neurogranin with neurodegenerative processes (see Xiang et al., 2020).

Zebrafish (*Danio rerio*) is a major model vertebrate for studies of developmental biology, including brain development, pharmacology, and neurobiology (Barros et al., 2008; Cassar et al., 2020; Eisen, 1991; Fulwiler & Gilbert, 1991; Schmidt et al., 2013). Adult zebrafish is also an important model for adult neuroanatomy, including a number of cytoarchitectonic and neurochemical studies (Barreiro-Iglesias et al., 2013; Castro et al., 2006a, 2006b, 2009; Kaslin & Panula, 2001; Kim et al., 2004; Mathieu et al., 2002; Mueller & Guo, 2009; Mueller et al., 2004; Wullimann et al., 1996; K. Yamamoto et al., 2010, Yamamoto et al., 2011) as well as hodological studies (Folgueira et al., 2020; Rink & Wullimann, 2004; Turner et al., 2016; Yáñez et al., 2017, 2018, 2021). Whereas the expression of different neurotransmitters (e.g., serotonin, dopamine, histamine, GABA, glycine), neurotransmitter-synthesizing enzymes (e.g., GAD, TH1, TH2, ChAT), and neuropeptides (e.g., GHRH, NPY) were the subject of various studies, regulatory proteins such as neurogranin have not been studied in the adult zebrafish brain. Thus, here we analyze *in silico* the sequences of the three neurogranin peptides predicted in zebrafish and compare them with those of other vertebrates. Western blot analysis, using a commercial neurogranin antiserum, confirms the presence of three "neurogranin-like" (Nrgn-like) peptides in zebrafish brain extracts, likely to be the products from paralog genes *nrgna* and *nrgnb* (Gómez et al., 2012; Wong et al., 2009; Zada et al., 2014). By immunohistochemical methods with the same antiserum, we describe the distribution of Nrgn-like immunoreactivity in the adult brain, olfactory organ, retina, and taste buds, showing that the expression is cell-type specific. Our results reveal some important differences between the distribution patterns reported in zebrafish and mammals, suggesting divergent evolution of the neurogranin systems of ray-finned fishes and land vertebrates from the last common ancestor.

2 | MATERIAL AND METHODS

2.1 | Animals

Wild-type zebrafish adults (*Danio rerio*) were kept in standard conditions (Aleström et al., 2020) at 28.0 ± 1.0°C and 14 h light/10 h dark periods. Fish were fed a mixture of dry flakes and *Artemia sp.* twice a day. All procedures were carried out following the Spanish Royal Decree 53/2013 and the European Union Directive 2010/63/EU regarding the protection of animals used for scientific research purposes.

2.2 | Neurogranin sequence analysis

Protein sequences for reedfish (bichir; *Erpetoichthys calabaricus*), zebrafish (*D. rerio*), Atlantic salmon (*Salmo salar*), spotted green pufferfish (*Tetraodon nigroviridis*), coelacanth (*Latimeria chalumnae*), xenopus (*Xenopus tropicalis*), green anole (*Anolis carolinensis*), easter brown snake (*Pseudonaja textilis*), zebrafinch (*Taeniopygia guttata*), platypus (*Ornithorhynchus anatinus*), rat (*Rattus norvegicus*) and human (*Homo sapiens*) neurogranins were obtained from Uniprot (www.uniprot.org) or Ensembl (https://www.ensembl.org/index.html) (Table 1). Protein sequences were aligned using NCBI Blastp (NIH; https://blast.ncbi.nlm.nih.gov/Blast.cgi) with the simplest adjustment ("composition-based

TABLE 1 Protein sequence identifiers for neurogranin in several vertebrates

Species	Sequence identifier	Length (aa)
Reedfish (*Erpetoichthys calabricus*)	Ensembl-ENSECRT00000017376.1	74
Zebrafish (*Danio rerio*)	UniProtKB-F6NQC4 (F6NQC4_DANRE)	60
	UniprotKB-F8W4I3 (F8W4I3_DANRE)	68
	UniProtKB-B7TWQ3 (B7TWQ3_DANRE)	92
	UniProtKB-A1L278 (A1L278_DANRE)	188
Atlantic salmon (*Salmo salar*)	UniProtKB-B5XEB8 (B5XEB8_SALSA)	94
Spotted green pufferfish (*Tetraodon nigroviridis*)	UniProtKB-H3BZW5 (H3BZW5_TETNG	84
Coelacanth (*Latimeria chalumnae*)	UniProtKB - H3ACE7 (H3ACE7_LATCH)	75
Xenopus (*Xenopus tropicalis*)	Ensembl-ENSXETG00000028009	495
Green anole (*Anolis carolinensis*)	Ensembl-ENSACAG00000025439	62
Easter brown snake (*Pseudonaja textilis*)	Ensembl-ENSPTXP00000015095	71
Zebrafinch (*Taeniopygia guttata*)	Ensembl-ENSTGUP00000034709	124
Platypus (*Ornithorhynchus anatinus*)	Ensembl-ENSOANP00000054267	73
Rat (*Rattus norvegicus*)	UniProtKB-Q04940 (NEUG_RAT)	78
Human (*Homo sapiens*)	UniProtKB - Q92686 (NEUG_HUMAN)	78

Neurogranin sequence identifiers and lengths (number of amino acids: aa) were taken from UniProt and Emsembl databases.

statistics"; Schäffer et al., 2001). Fully conserved amino acids (aa) were marked with an asterisk (*), groups of strongly similar properties with a colon (:), and weakly similar properties with periods (.). The IQ domain (20 aa; AAAAKIQASFRGHMARKKIK) was annotated manually following the sequence described by Prichard et al. (1999).

2.3 | Western blot assay

Brains (80 mg) and spleens (10 mg) of five adult zebrafish were mechanically homogenized separately in lysis buffer solution (pH 7.6) containing 50 mM Tris, 5 mM EDTA, 5 mM 2-mercaptoethanol, 150 mM NaCl, and a complete protease inhibitor (Thermo Scientific™, PI88266). The homogenized tissues were then centrifuged at 4°C (12,000 rpm; 5 min). Proteins and peptides in the supernatant were centrifuged again for 40 min in the same conditions. Finally, supernatant of this fraction was collected, and total protein concentrations were determined using the Protein Assay Dye Reagent Concentrate (Bio-Rad, #5000006). Supernatants were aliquoted and stored at −20°C until further used.

After defrosting the aliquots, proteins and peptides were denatured for 5 min at 90°C and separated by sodium dodecyl sulfate polyacrylamide gel electrophoresis (SDS–PAGE). For this, 10–20 μg of protein in 4× sample buffer (Sigma-Aldrich, G2526) was applied to each lane of a 16% polyacrylamide gel. A standard molecular weight marker (Spectra Multicolor Broad Range Protein Ladder 10–260 kDa; ThermoFisher Scientific, Product #SM26634) was also included in an additional lane. A constant electric current of 100 V was then applied to the gel for 2 h (Mini-Protean II PAGE system, Bio-Rad, Richond, CA, USA). Homogenates of Wistar rat (*R. norvegicus*) and gray mullet (*Chelon labrosus*) brains, prepared for previous studies (Lamas et al., 2007), were subjected to identical protocol. Separated proteins and peptides were then electroblotted onto a nitrocellulose membrane (0.2 μm pore size; Bio-Rad 162-0146, #G5961143) at 100 V for 1 h.

For immunoblotting, nonspecific binding sites were blocked by incubation in 5% milk powder in 0.01 M saline phosphate buffer (PBS; 0.14 M NaCl, pH 7.4) with 0.2% Tween-20 (PBS-MT) overnight at 4°C. Then, membranes were incubated with anti-Nrgn antiserum (Rabbit Anti-Neurogranin Polyclonal Antibody, Chemicon, AB5620, Lot #3091673) in PBS-MT (1:1000 dilution) overnight at 4°C. According to the supplier, this antibody was generated in rabbits against the complete sequence of recombinant rat neurogranin. Next, membranes were washed three times (10 min each) in PBS-MT and then incubated for 1.5 h at room temperature with goat-anti-rabbit IgG antibody conjugated to horseradish peroxidase (Sigma Aldrich, A9169, Lot #023M4757, 1:800 dilution) in PBS-MT. After three rinses in PBS-MT, antibody bindings were visualized by incubation in diaminobenzidine (Sigma-Aldrich, 077K36641) with 0.001 % hydrogen peroxide in PBS for 5–10 min at room temperature, intensified with 0.03 % cobalt chloride.

2.4 | Immunohistochemistry

For immunohistochemical assays, nine adult zebrafish were euthanized in 0.1% ethyl 3-aminobenzoate methanesulfonate (MS-222) and next perfused with 4% paraformaldehyde (PFA) in PBS. After perfusion, brains, retinas, olfactory organs, and one oral barbel were dissected out and postfixed overnight in the same fixative at room temperature. Then, samples were rinsed in PBS and kept at 4°C until use.

For immunocytochemistry in cryosections, brains and retinas were cryoprotected in 30% sucrose in phosphate buffer (PB; 0.1 M pH 7.4)

overnight at 4°C. Then, brains, olfactory organs, and retinas were embedded in Tissue-TEK OCT medium (Sakura Finetek, Torrance, CA, USA) and frozen by immersion in liquid nitrogen-cooled methyl butane. Blocks were stored at −20°C until sectioning in a cryostat (transverse sections; 12 μm thick). In order to perform the immunostaining, sections were first incubated in 0.2% sodium borohydride in PBS (30 min). Nonspecific binding sites were blocked by incubating sections in 10% normal goat serum (Sigma Aldrich, G6767-19B409) in 0.5% Triton-X-100 in 0.1 M PBS (PBST; pH 7.4) for 1 h. Sections were then incubated overnight at 4°C with the neurogranin antiserum (Rabbit Anti-Neurogranin Polyclonal Antibody, Chemicon, AB5620, Lot#3091673, 1:500–1:750 dilution). For immunofluorescence, samples were incubated with Alexa Fluor 488-coupled goat anti-rabbit IgG antibody (Sigma Aldrich, A11008, 1:500 dilution) for 1 h at room temperature. Slides were mounted using 50% glycerol in PB.

For immunofluorescence in vibratome sections, fixed brains and retinas were embedded in 3% agarose and sectioned using a vibratome (Vibroslice, Campden Instruments, UK; 50–60 μm thick). Then, transverse sections were transferred to small Eppendorf tubes and stored overnight in 100% methanol at −20°C. Sections were rehydrated, washed three times (5 min each) in PBST, permeabilized with proteinase K in PBS (20 min; Sigma Aldrich, P2308), and then postfixed with 4% PFA (20 min). After three washes in PBST (10 min each), sections were incubated with 10% normal goat serum (Sigma Aldrich, G6767-19B409) in PBST for 1 h. Then, sections were incubated with the primary antibody solution (Rabbit Anti-Neurogranin Polyclonal Antibody; Chemicon, AB5620, Lot#3091673, 1:500 dilution) for 3 days at 4°C. After, sections were washed four times (30 min each) and incubated with Alexa Fluor 488-coupled goat anti-rabbit antibody (Sigma Aldrich, A11008, 1:500 dilution) overnight at 4°C. Sections were washed in PBST (30 min) and mounted on gelatinized slides with 50% glycerol in PB for imaging. The oral barbel of an adult zebrafish and the trunk of two specimens of 5 days old were also processed in toto in a similar way as the vibratome sections.

As complementary material, paraffin sections of two additional adult zebrafish were also used for double immunolabeling against neurogranin and zebrin II monoclonal antibody (hybridoma supernatant from Prof. Hawkes, dilution 1:100; see also Lannoo et al., 1991a, 1991b).

Sections of adult zebrafish brains and retinas were analyzed with an Epifluorescence microscope (Nikon Eclipse 90i) coupled to Olympus DP71 digital camera. The maxillary barbel was also imaged using a laser scanning confocal microscope Nikon A1R equipped with Nikon Plan Fluor 20× (0.50 NA) objective lens.

3 | RESULTS

3.1 | Comparative sequence analysis of the neurogranin polypeptide

Zebrafish have two neurogranin paralog genes: *nrgna* (ZFIN ID: ZDB-GENE-090710-4; Zada et al., 2014) and *nrgnb* (ZFIN ID: ZDB-GENE-070112-1912; *spa17* in Gómez et al., 2012; "neurogranin-similar" in Wong et al., 2009) located in chromosomes 5 and 15, respectively. From these two genes, four peptides of different lengths have been predicted based on evidence at a transcript or sequence level: (a) from *nrgna*, three isoforms of 60 aa (sequence identifier: UniProtKB-F6NQC4), 68 aa (UniprotKB-F8W4I3), and 92 aa (UniProtKB-B7TWQ3); (b) from *nrgnb*, a peptide of 188 aa (UniProtKB-A1L278). The transcript for the 68 aa peptide seems to be susceptible to "nonsense-mediated decay" (see Emsembl), so it is not likely to be translated (Karousis & Mühlemann, 2019). Thus, the two neurogranin genes in zebrafish seem to translate into three peptides, referred to here onwards as Nrgna-60, Nrgna-92, and Nrgnb-188.

(a)

	Nrgna-92	Nrgnb-188	*Tetraodon nigroviridis*	*Salmo salar*	*Rattus norvegicus*
Nrgna-60	100 %	82.14 %	83.33 %	83.02 %	66.67 %
Nrgna-92	-	82.14 %	83.33 %	83.02 %	68.09 %
Nrgnb-188	-	-	81.97 %	81.91 %	80.65 %

(b)

```
                                                        IQ domain
Erpetoichthys calabricus  ----------MDCSSEDCNKQQD-EEVLDIPLDDPEANKAAKIQA S FRGHMTRKKIKS  48
Danio rerio (Nrgn-60 aa)  ----------MDCRNEGCSQPQD-EDIMDIPLDDPAANKAAKIQA G FRGHMTRKKMKD  48
Danio rerio (Nrgn-92 aa)  SNFTKLSSPIAMDCRNEGCSQPQD-EDIMDIPLDDPAANKAAKIQA G FRGHMTRKKMKD  80
Danio rerio (Nrgn-188 aa) ----------MDCHIEECSQPQEEEDIMDIPLDDPEANKAAKIQA G FRGHMTRKKMKP  49
Salmo salar               ----------MDCHIEECSQPQEEEDIMDIPLDDPEANKAAKIQA G FRGHMTRKKIKP  49
Tetraodon nigroviridis    ----------MDCHNEDCSRPQEEEDIMDIPLDDPEANRAAKIQA G FRGHMTRKKLKP  49
Latimeria chalumnae       ----------RCRNKEETCTKLD--KDILDPLDDPDANAAAKIQA N FRGHMTRKKIKE  48
Xenopus tropicalis        VLEHEDRSNLESPKENESFRKPQ--EEALDIPLDDPDANAAAKIQA G FRGHMTRKKMKG  472
Anolis carolinensis       ----------MDCCNEGACTKLD--EDILDPLDDPDANAAAKIQA S FRGHMTRKKIKG  48
Pseudonaja textilis       -----------IFCCNSCTKLD--EDILDPLDDPDANAAAKIQA S FRGHMTRKKIKG  46
Taeniopygia guttata       PAAVWSRVGFRNEWEEGACTKLD--EDILDPLDDPDANAAAKIQA S FRGHMTRKKIKG  99
Ornithorhynchus anatinus  --------------ESACSKPD--DDILDPLDDPGANAAAKIQA S FRGHMARKKIKS  43
Rattus norvegicus         ----------MDCCTESACSKPD--DDILDPLDDPGANAAAKIQA S FRGHMARKKIKS  48
Homo sapiens              ----------MDCCTENACSKPD--DDILDPLDDPGANAAAKIQA S FRGHMARKKIKS  48
                                     : :  .: :******* ** ******* .  *****:***:*
```

FIGURE 1 (a) Results of NCBI Blastp showing amino acid identity (%) of full-length sequences of neurogranin from rat (*R. norvegicus*), spotted green pufferfish (*T. nigroviridis*), Atlantic salmon (*S. salar*), and zebrafish (*D. rerio*) variants a (derived from *nrgna* > Nrgna-60 and Nrgna-92) and variant b (*nrgnb* > Nrgnb-188). (b) Alignment of neurogranin sequences containing IQ domain between organisms. Right column indicates the position of the last amino acid shown in the selected portion of the whole sequence. Twenty-five amino acids were fully conserved (*), six amino acids were strongly similar (:) and only two amino acids were weakly similar (.). IQ domain is highly conserved in all sequences [16 (*), 2 (:), and 1 (.)]. Serine (S) located in position 36 (outlined box) in basal actinopterigyans (*E. calabaricus*), reptiles, birds, and mammals, is substituted by glycine (G) in teleosts and *X. tropicalis*, and by asparagine (N) in sarcopterygii (*L. chalumnae*)

The alignment of the deduced zebrafish neurogranin sequences (Nrgna-60, Nrgna-92, and Nrgnb-188) with homolog sequences in other species is shown in Figure 1. Overall, zebrafish neurogranin sequences show a high degree of conservation (Figure 1a), with Nrgnb-188 having the highest identity with the rat. Manual annotation showed that all zebrafish predicted peptides contain an IQ domain with over 80% amino acid identity (Figure 1b).

We compared the IQ domain of zebrafish with that of other species of actinopterygians (*Erpetoichthys calabricus*, *S. salar*, and *T. nigroviridis*), sarcopterygians (*L. chalumnae*), amphibian (*X. tropicalis*), reptiles (*A. carolinensis* and *P. textilis*), bird (*T. guttata*), and mammals (*O. anatinus*, *R. norvegicus*, and *H. sapiens*). This showed differences in position 36, which is phosphorylated by PKC in mammals (Baudier et al., 1991; Díez-Guerra, 2010; Domínguez-González et al., 2007; Gerendasy & Sutcliffe, 1997; Huang et al., 1993; Koob et al., 2014; Yang et al., 2015).

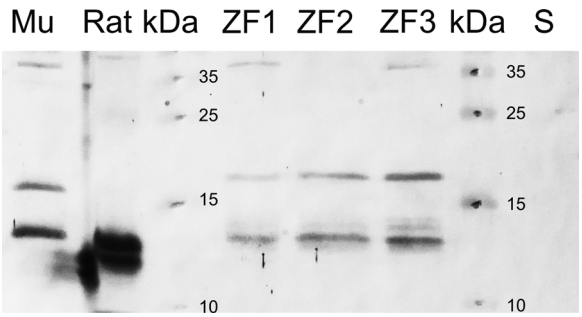

FIGURE 2 Western blot results for the different protein homogenates employed from zebrafish (ZF and S), Wistar rat (Rat) and gray mullet (Mu). Two zebrafish brain extracts (ZF1 and ZF3) show three Nrgn-ir bands of about 13, 20 and 37 kDa. Note the absence of the 37-kDa band in the zebrafish brain extract lacking the telencephalic lobes (ZF2). In zebrafish spleen homogenate (S), no Nrgn-ir bands were observed. Immunoblotting with anti-Nrgn-antiserum was also analyzed in parallel in brain extracts of Wistar rat (*R. norvegicus*) and gray mullet (Mu; *C. labrosus*)

A glycine (G) is present in this position in teleosts and *Xenopus*, while an asparagine (N) is present in *Latimeria* and a serine (S) in cladistians (basal actinopterygians), reptiles, birds, and mammals (Figure 1b).

3.2 | Western blot analysis

We investigated the specificity of the neurogranin primary antibody used in this study by western blot analysis with brain homogenates of adult zebrafish, rat and gray mullet (Figure 2). In addition, zebrafish spleen homogenates were also used (Figure 2). In the rat lane (Ra), we observed a band of around 14 kDa that matches results from previous studies (Baudier et al., 1989, 1991; Represa et al., 1990; Watson et al., 1990, 1992). In the case of the zebrafish brain, our results revealed three different bands of approximately 13, 20 and 37 kDa in two homogenates (ZF1 and ZF3). Based on their predicted molecular mass and neurogranin behavior in SDS–PAGE (Baudier et al., 1989, 1991; Coggins et al., 1993; Deloulme et al., 1991; Díez-Guerra, 2010; Tejero-Díez et al., 1999), these three bands seem to correspond to the three polypeptides of 60 aa, 92 aa, and 188 aa predicted for zebrafish. One brain homogenate (ZF2), which did not contain the telencephalon, did not reveal the 37-kDa band. In zebrafish spleen homogenate (S), we did not observe any labeled band. Similar to zebrafish, we also observed three bands of about 12, 19, and 39 kDa in the gray mullet protein extract (Mu) (Figure 2). Our results indicate that the primary antibody used here, raised against rat neurogranin, cross-reacts with zebrafish, and gray mullet neurogranin or "Nrgn-like" proteins.

3.3 | Neurogranin expression in the brain and sensory organs

In the adult zebrafish, the presence of Nrgn-like immunoreactivity was studied in an entire oral barbel and sections of the olfactory organ, retina and brain. We observed immunoreactivity mainly located in the cytosol of cell bodies, sometimes extending along thick dendrites, but also in fiber bundles and axon terminals (Figures 3–8). In the brain, all positive cells were putatively identified as neurons, whereas the ependymoglia (the most abundant and easily identifiable macroglial cell type in zebrafish and other teleosts) was always Nrgn-like negative. Since no experiment with double labeling of neurogranin with oligodendrocyte markers was performed, we cannot rule out the possibility that some cells were oligodendrocytes, although positive

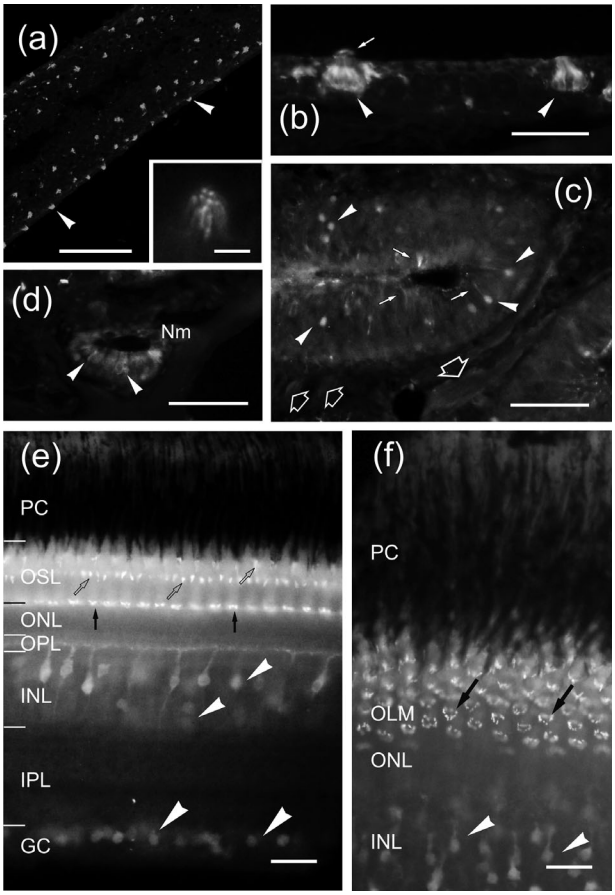

FIGURE 3 (a–d) Nrgn-like distribution in the surface of a barbel (a), skin (b), the olfactory organ (c) and the retina (e, f). (a) Nrgn-like immunoreactivity in the apical region of sensory cells in taste buds (arrowheads); detailed in the inset. (b) Transverse section of two Nrgn-like immunoreactive taste buds (arrowheads) at the dorsal surface of the head. Arrow points to apical microvilli. (c) Transverse section of the olfactory rosette showing Nrgn-like-ir in cell bodies (arrowheads) and apical dendrites (arrows) of olfactory receptor cells. Note the very low immunoreactivity in the olfactory axon bundles (open arrows). (d) Detail of a supraorbital canal neuromast showing weak Nrgn-like immunoreaction in hair cells (arrowheads). (e) Vertical section of the retina showing Nrgn-like-ir cell bodies (arrowhead), puncta (black arrows) and comma-like structures (white arrows). (f) Oblique section through the retina showing Nrgn-like-ir cell bodies in the INL (arrowheads) and details of the Nrgn-like-ir puncta arranged in a ring pattern around the base of the inner segment of photoreceptors (black arrows). For abbreviations, see the list. Scale bars: 100 μm (a–c), 50 μm (b,d), 25 μm (e–f), and 10 μm (inset in a)

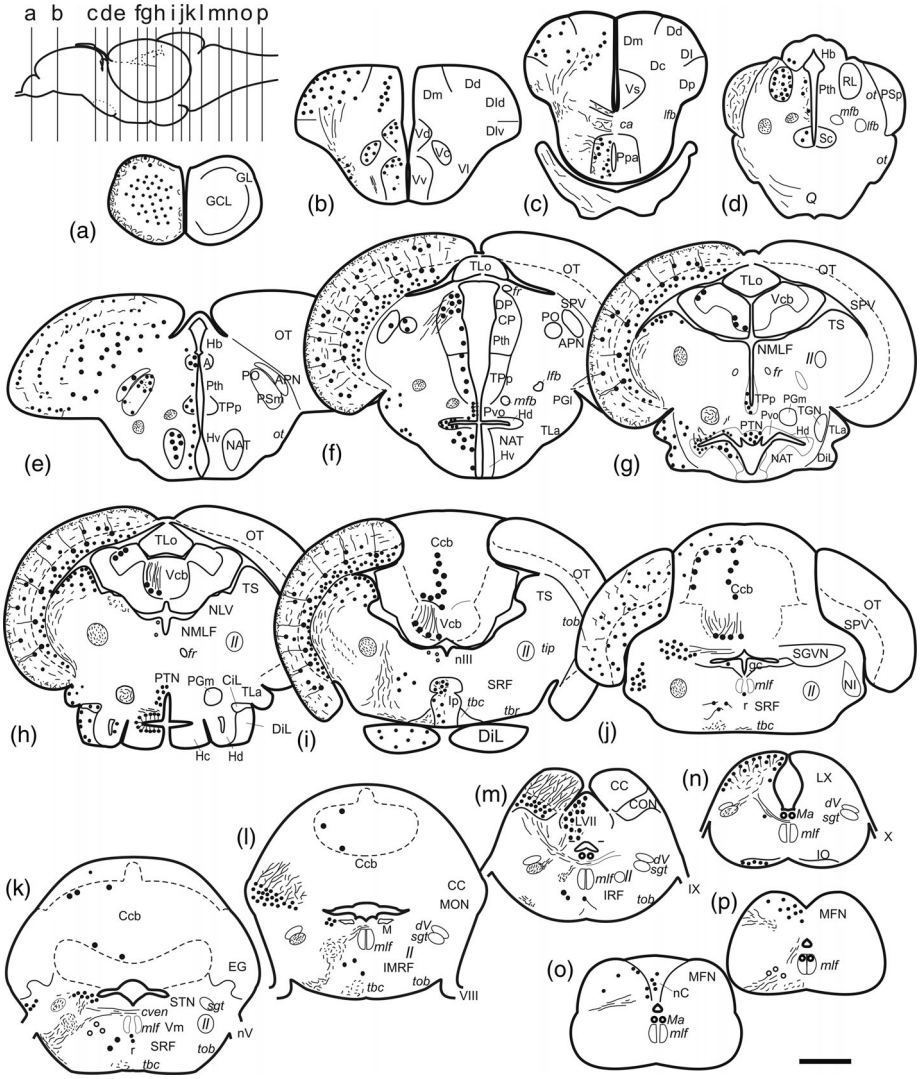

FIGURE 4 (a–p) Schematic drawings of transverse sections of the zebrafish brain from rostral (a) to caudal (p) showing on the left the Nrgn-like-ir cell bodies (big dots), neuronal processes and tracts (thin lines and small dots), while on the right the annotations of different nuclei and tracts. The levels of the sections are indicated by lines in the lateral diagram of the brain on the left. For abbreviations, see the list. Scale bar for sections: 200 μm (a–p)

cells were lacking in the major white matter tracts where oligodendrocytes typically abound in teleosts (Díaz-Regueira & Anadón, 1998). In one specimen, grainy fluorescence was observed in some endothelial cells (not shown).

3.3.1 | Chemosensory organs

Nrgn-like immunoreactive (-ir) cell bodies were observed in taste buds of the oral barbel and in the olfactory organ of the adult zebrafish. Taste buds in zebrafish are distributed in the mouth and oropharyngeal cavities and the skin of the head, lips, oral barbels, and other regions of the body (Hansen et al., 2002). Of all these, we analyzed only the maxillary barbels present in a sexually mature fish. We observed Nrgn-like immunoreactivity in apical dendrites of some taste cells (6–10 cells in each taste bud) (Figure 3a,b).

In the olfactory organ, goblet cells located peripherally in the non sensory epithelium of the olfactory lamellae appeared intensely immunolabeled. In the sensory epithelium, weak Nrgn-like immunoreactivity was observed in bipolar cell bodies located at basal and intermediate levels, and in some apical dendrites. In addition, very low immunoreactivity was observed in axon bundles of the olfactory nerve coursing under the epithelium (Figure 3c).

3.3.2 | Mechanosensory organs

Although a search was made only along the head of the adult zebrafish, Nrgn-like-ir cells were observed in hair cells of cranial canal neuromast (Figure 3d). No Nrgn-like immunoreactive superficial neuromasts of the lateral line could be confirmed in the 5-day-old larvae analyzed *in toto*.

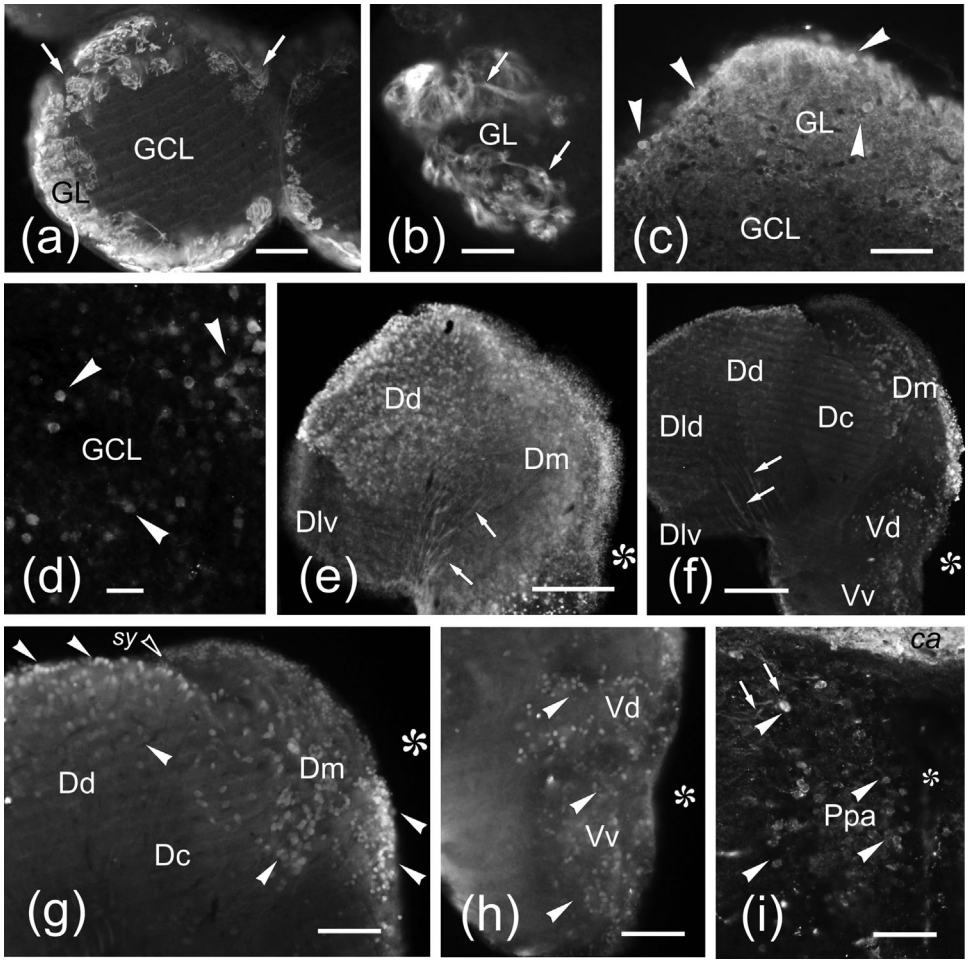

FIGURE 5 (a–i) Photomicrographs of transverse sections of the olfactory bulb (a–d), telencephalic lobes (e–h) and preoptic area (i) of the zebrafish brain showing Nrgn-like-ir cell bodies (arrowheads) and fibers (arrows). Medial is to the right. (a) General view of a vibratome section of the olfactory bulb showing Nrgn-like-ir fibers in the glomerular layer. (b) Detail of an olfactory glomerulus showing Nrgn-like-ir fibers. (c) Detail of a cryostat section showing Nrgn-like-ir cell bodies in the glomerular layer. (d) Detail of Nrgn-like-ir granule cells. (e) General view of a telencephalic lobe at the rostral level. (f) Vibratome section of a telencephalic lobe at precommissural level. (g) Detail of a vibratome section showing Nrgn-like-ir cell bodies. Note the absence of labeled cell bodies in the Dlv and Dc. (h) Vibratome section through the subpallium showing positive cell bodies in Vd and Vv. (i) Detail of positive cell bodies in the anterior parvocellular preoptic region (Ppa). Asterisk, ventricle. For abbreviations, see the list. Scale bars: 200 μm (e–f), 100 μm (a, g–h), 50 μm (b,c, i), and 20 μm (d)

3.3.3 | Retina

In the adult retina, Nrgn-like-ir cells were identified as bipolar, amacrine and ganglion cells (Figure 3e). In these cells, Nrgn-like immunoreactivity seems to be located in the cytosol, labeling the whole cell. Nrgn-like-ir bipolar cells showed a characteristic morphology: a fusiform cell body extending a thick apical dendrite that branches in the outer plexiform layer and a thin axon that branches in the inner plexiform layer (IPL) (Connaughton et al., 2004). By their morphology, most of these cells probably correspond to rod bipolar cells. Cells identified as amacrine neurons showed weakly labeled round cell bodies located in the proximal tier of the inner nuclear layer (INL). A number of ganglion cell somas were faintly labeled in the ganglion cell layer, although no immunoreaction could be observed in the optic fiber layer. At the level of the outer limiting membrane, we observed aggregates of 7–12 brightly fluorescent puncta that are arranged in a round pattern, located at the base of the myoid of the inner segment of the short-single ultraviolet-wavelength sensitive cones (UV cones) of the adult retina (see Robinson et al., 1993; Salbreux et al., 2012; Takechi et al., 2003). Furthermore, barrels of comma-like structures were also labeled associated with the base of the inner segment of long outer cones (Figure 3f).

3.3.4 | Brain

Telencephalon, preoptic area, and hypothalamus (secondary prosencephalon)

In the olfactory bulbs, Nrgn-like immunoreactivity was observed mostly in olfactory fibers located in the dorsal and ventrolateral

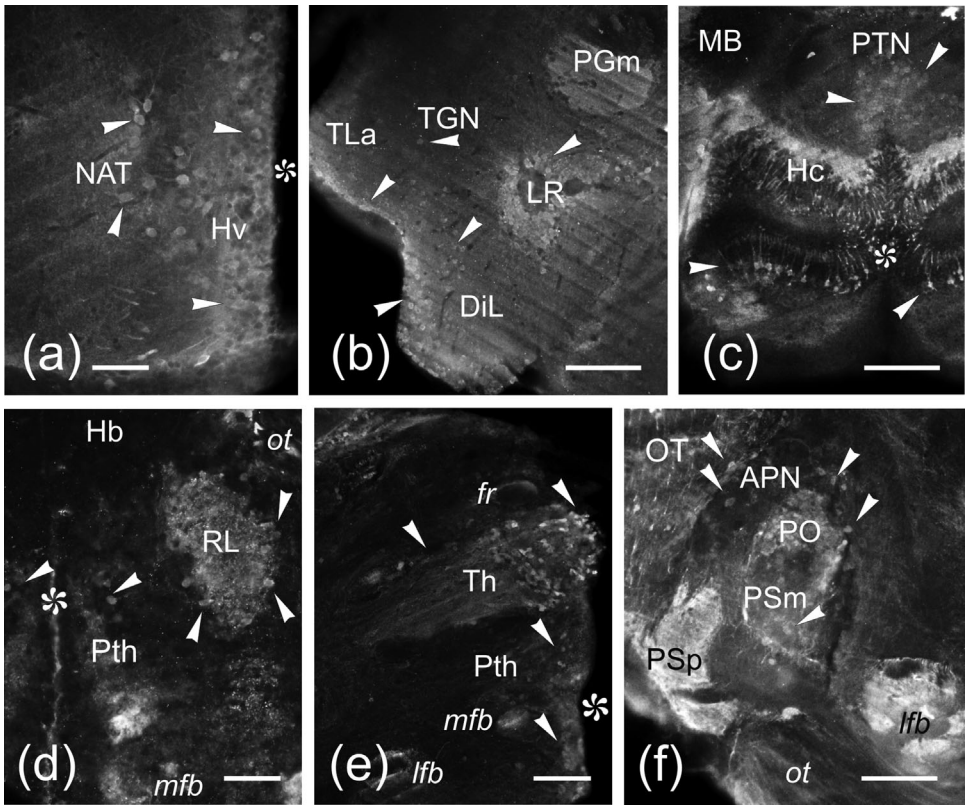

FIGURE 6 (a–f) Vibratome (a–c, e–f) and cryostat (d) cross sections of the zebrafish brain through the hypothalamus (a,b) and diencephalon (c–f), showing Nrgn-like-ir labeled cell bodies (arrowheads) and processes (arrows). Medial is to the right. (a) Section through the rostral hypothalamic region showing lightly labeled Nrgn-like-ir cell bodies in the NAT. (b) Detail of the lateral inferior lobe showing immunopositive cells in the torus lateralis (TLa), diffuse nucleus (DiL) and around the lateral recess (LR). (c) Detail of Nrgn-like-ir immunoreaction in the posterior lobe. (d) Section showing immunoreactive cell bodies in the nucleus rostrolateralis (RL). (e) Section through the thalamus. (f) Detail of the pretectal area. Asterisk, ventricle. For abbreviations, see the list. Scale bars: 100 μm (b,c, e–f), 50 μm (a,d)

glomeruli (Figures 4a and 5a,b). In some cryostat sections, some Nrgn-like-ir round cell bodies were also seen at the margin of the olfactory bulb among the immunoreactive processes (Figure 5c). Occasionally, larger positive somas were also observed within the glomerular layer. Also in cryostat sections, cytoplasmic Nrgn-like immunoreaction was observed in a number of small cells of the granular layer (Figures 4a and 5d).

In the pallium (dorsal telencephalic area, D) (Figures 4b,c and 5e–h), Nrgn-like-ir cell bodies were mostly observed in the periventricular region, but also sparsely distributed in deeper areas of the dorsal (Dd) and lateral (Dl) zones and, but not exclusively, in the ventral area of the medial zone (Dm). In cryostat sections, no positive cells were observed in the posterior zone of D (Dp), although it was traversed by Nrgn-like-ir bundles of the lateral telencephalic tract. In addition, at the level of the anterior commissure, Nrgn-like positive cell bodies and fibers were also observed in the central zone of D (Dc). Note that these zebrafish pallial zones correspond to those described in Yáñez et al. (2021).

In the subpallium (ventral telencephalic area, V) (Figures 4b,c and 5f–h), some Nrgn-like-ir perikarya were observed in the dorsal (Vd) and central (Vc) nuclei, as well as a few faintly labeled cells dorsally in the ventral nucleus (Vv). At precommissural levels, Nrgn-like-ir fiber bundles mainly originating from Dd converge in the lateral telencephalic tract, which courses along the lateral margin of subpallium. In the same region, a few Nrgn-like-ir cells were observed in the lateral nucleus of V (Vl). At commissural levels, Nrgn-like-ir fibers of the lateral forebrain bundle decussate at the anterior commissure (*ca*) (Figure 4c).

In the preoptic area, Nrgn-like immunoreactivity was seen in many cells located periventricularly in the anterior part of the parvocellular preoptic nucleus (Ppa) and also deeper in some larger neurons that send their processes laterally (Figures 4c and 5i). Occasional Nrgn-like-ir cells were also observed in the magnocellular preoptic nucleus (Ppm). A few Nrgn-like-ir cells could be also observed in the suprachiasmatic nucleus (Figure 4d).

In the hypothalamus, abundant Nrgn-like-ir cell bodies displaying cerebrospinal fluid-contacting (CSF-c) morphology were observed in the paraventricular organ (Pvo) and posterior recess organ (Figures 4f,g and 6c). Moreover, a dense mat of Nrgn-positive fibers is closely associated with these organs, probably formed by the axons of these cells. Nrgn-like-ir cells were also observed in the anterior tuberal nucleus (NAT) and the ventral (Hv) and dorsal (Hd) nuclei of the periventricular hypothalamus (Figures 4e,f and 5a,c). Scattered Nrgn-like-ir cell bodies could also be observed mainly in the torus lateralis (TLa), and the

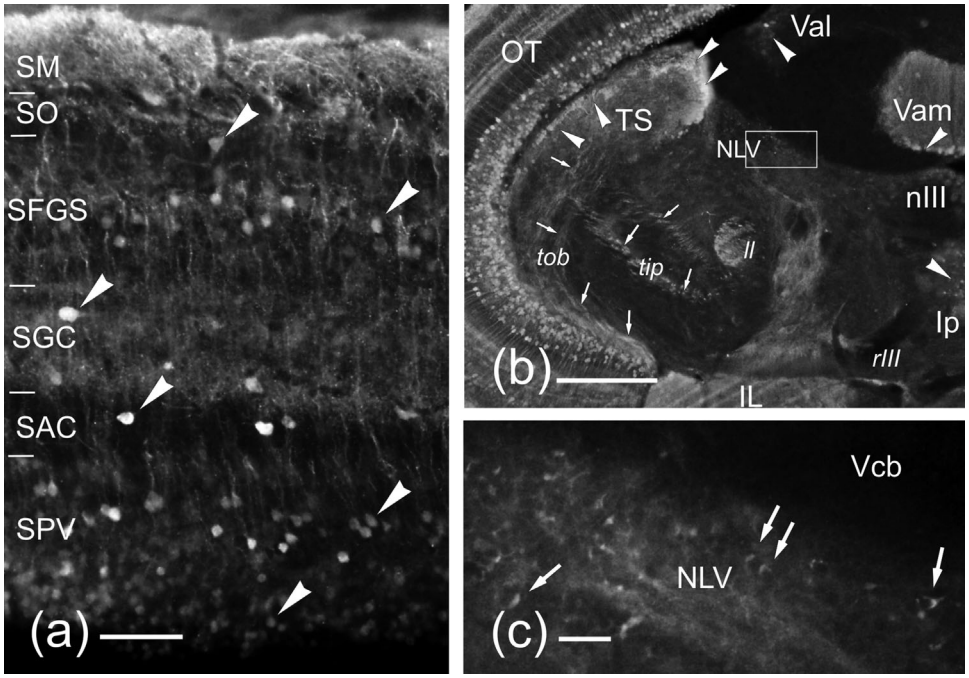

FIGURE 7 (a–c) Photomicrographs of transverse sections through the mesencephalon of the zebrafish showing Nrgn-like-ir immunoreaction in cell bodies (arrowheads) and processes (arrows). (a) Cross section through the OT showing immunoreactive cell bodies (arrowheads). Note the SM is crowded with immunoreactive dendritic branches. (b) Transverse vibratome section through the mesencephalic tegmentum. The midline is to the right. (c) Detail of Nrgn-like-ir axonal endings (arrows) in the NLV. For abbreviations, see the list. Scale bars: 200 μm (b), 50 μm (a), 20 μm (c)

diffuse (DiL) and central (CiL) nuclei of the hypothalamic inferior lobes (Figures 4e–i and 6a–c). A few positive cell bodies were seen in the region of the tertiary gustatory nucleus (TGN) proper sense of Yáñez et al. (2017) (Figures 4 g and 6b) (see the Discussion).

Diencephalon

In the dorsal (alar) region of the diencephalon, some Nrgn-like-ir fibers and a few periventricular cell bodies were located in the prethalamus (Pth; formerly ventral thalamus) (Figures 4d–f and 6d,e). The nucleus rostrolateralis (RL), considered epithalamic by Saidel (2013), showed many Nrgn-like-ir cell bodies and fibers (Figures 4d and 6d). In the epithalamus, many positive cell bodies were observed along the pineal tract and in the parapineal organ (not shown). In the habenulae (Hb), a few faintly Nrgn-like-ir cell bodies were scattered in the ventral nucleus (Figure 4d,e). In the thalamus (Th; formerly dorsal thalamus), Nrgn-like-ir cells were located in the anterior (A) and dorsal posterior thalamic nuclei (Figures 4d–f and 6d–f). In the pretectal area, the parvocellular superficial pretectal nucleus (PSp) showed a number of Nrgn-like-ir fibers, whereas the accessory pretectal nucleus (APN) and magnocellular superficial (PSm) pretectal nuclei showed some Nrgn-like-ir cell bodies. The posterior pretectal nucleus (PO) showed both Nrgn-like-ir cell bodies and fibers (Figures 4d–f and 6f).

In the ventral (basal) diencephalic region, some Nrgn-like-ir cell bodies were observed in the ventral part of the periventricular nucleus of the posterior tubercle (TPp), the medial preglomerular nucleus (PGm), and a few periventricular Nrgn-like-ir cell bodies in the posterior tuberal nucleus (Figures 4e–h and 6b,c). In addition, both the lateral (*lfb*) and the medial (*mfb*) forebrain bundles showed Nrgn-like-ir fibers (Figures 4c–f, 5e,f, and 6e,f). Caudally, a few cell bodies were faintly immunostained in the nucleus of the medial longitudinal fascicle (Figure 4h).

Mesencephalon

In the alar region of the mesencephalon, numerous Nrgn-like-ir cell bodies were observed in the optic tectum (OT), and in lesser proportion in the torus semicircularis (TS) (Figures 4e–j and 7a,b). In the OT, many round or piriform cell bodies were found in the stratum periventriculare (SPV), which appeared organized in two separated depths (Figure 7a): (1) one periventricular band of four to six rows of pale Nrgn-like-ir cell bodies and (2) another apical thinner band of one to three rows of more intensely stained cell bodies next to the stratum album centrale (SAC). Most neurons of the latter band showed a long apical radial dendrite and likely correspond to type XIV cells of Meek and Schellart (1978). In addition, some Nrgn-like-ir cell bodies were observed in the stratum fibrosum griseum superficiale (SFGS), a few in the stratum griseum centrale (SGC), and occasionally in the SAC. The cell bodies of the SGC and SFGS are round or fusiform, with a thick apical dendrite branching profusely in the stratum marginale (SM). Thus, these cells appear to correspond with pyramidal cells (Laufer & Vanegas, 1974; Vanegas et al., 1974) or type I cells of Meek and Schellart (1978). Nrgn-like-ir fibers were distributed in the stratum opticum, in the SFGS, and three sublaminae in the SGC (Figure 7a). No

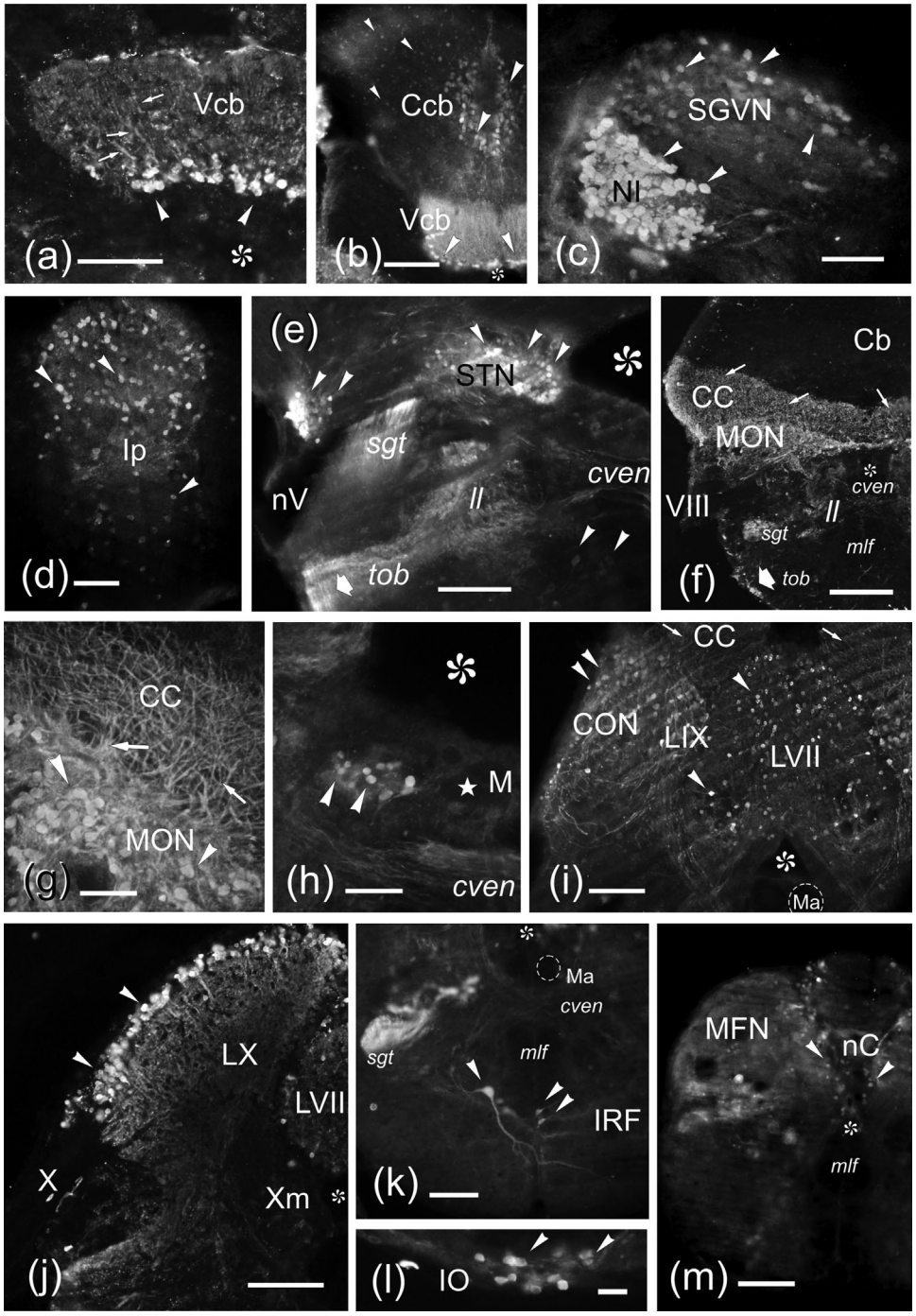

FIGURE 8 (a–m) Photomicrographs of transverse sections of the zebrafish rhombencephalon showing Nrgn-like-ir cell bodies (arrowheads) and processes (arrows). Medial is to the right except in (d). (a,b) Nrgn-like-ir in Purkinje cells in the medial division of the valvula (a, b) and corpus (b) of the cerebellum. Only in the cerebellar valvula (Vcb) the apical dendrites of these cells (arrows) can be well observed. (c) Detail of the NI and the secondary gustatory-visceral nucleus (SGVN) showing intensely and lightly labeled immunoreactive cell bodies, respectively. (d) Detail of the interpeduncular nucleus (Ip). (e) Nrgn-like-ir neurons in the sensory nucleus of the trigeminal nerve (STN) and dorsal to the sensory root entrance of the trigeminal nerve (nV). (f) General view of a cryostat section at the level of the octaval nerve (VIII) entrance. Note the high amount of Nrgn-like-ir dendrites in the CC and the Nrgn-like-ir in two fiber bundles, the secondary gustatory tract (*sgt*) and the bundle at the ventrolateral margin of the tegmentum (thick arrow). (g) Vibratome cross section showing a detail of the Nrgn-like-ir cells of the MON. (h) Vibratome section showing a discrete group of Nrgn-like-ir cells close to the Mauthner cell. (i) Nrgn-like-ir cells (arrowheads) in the caudal octavolateral region and the viscerosensory lobes (IX, VII). Note the Nrgn-like-ir dendrites of the CON (arrows) entering the CC. (j) Detail of the vagal lobe showing Nrgn-like-ir cell bodies mostly at its periphery. (k) Vibratome cross section at the level of the inferior reticular formation showing immunoreactivity in a large reticular cell and a couple of small cells. Note also the *sgt* intensely labeled. (l) Detail of Nrgn-like-ir cell bodies in the IO. (m) Section at the level of the commissural nucleus of Cajal (nC). Asterisk, ventricle. For abbreviations, see the list. Scale bars: 500 μm (f), 200 μm (k, m), 100 μm (a,b,e, i,j), 50 μm (c,d, g,h),and20 μm (l)

Nrgn-like immunoreactivity was observed in the torus longitudinalis (TLo), located along the medial border of the OT.

In the TS, most Nrgn-like-ir cell bodies were observed in a periventricular location (Figure 7b). Nrgn-like-ir tracts reach the TS running between the OT and the tegmentum.

In the basal mesencephalon, Nrgn-like immunoreactivity was observed mainly in fiber tracts. Light immunoreactivity was also seen in cell bodies of the oculomotor nucleus (nIII) region (Figures 4i and 7b). However, no immunoreactivity was seen in the oculomotor nerve root or the medial longitudinal fascicle. In the precerebellar lateral valvular nucleus (NLV), thick Nrgn-like-ir fiber endings, at least some of them showing a cup- or basket-shaped morphology, were observed around cells of this nucleus (Figures 4h and 7b,c). Based on present results, part of these fibers may come from the ipsilateral hypothalamic lobe, as loose bundles of Nrgn-like-ir fibers were observed connecting the lateral lobes of the hypothalamus and the mesencephalic tegmentum (Figures 4i and 7b). Moreover, Nrgn-like-ir fibers were observed in the lateral lemniscus (*ll*), the torobulbar tracts, the isthmo-pretectal tract (*tip*) of Yáñez et al. (2017) (see the Discussion), and in the tectobulbaris rectus (*tbr*) and cruciatus (*tbc*) tracts (Figures 4 g and 7b) that course caudally.

Rhombencephalon

In the cerebellum, very intense Nrgn-like immunoreactivity was observed in large cell bodies of the medial (Vam) and lateral (Val) divisions of the cerebellar valvula (Vcb) (Figures 4 g–l, 7b, and 8a–e). However, only in the medial valvula the characteristic thick dendrites of Purkinje cells, branching into the molecular layer, were clearly immunostained (Figures 7h–j and 8a,b). In the cerebellar corpus (Ccb), fairly numerous large cell bodies also showed Nrgn-like immunofluorescence (Figures 4i–k and 8b). Double immunostaining against the specific Purkinje cell marker "zebrin II" (see Bae et al., 2009) and neurogranin confirmed colocalization of both markers in many cells, indicating that they were Purkinje cells. In the absence of double immunostaining experiments with markers for eurydendroid cells, we cannot rule out the possibility of neurogranin expression in these cells. In the rostral part of the cerebellar corpus of one specimen, small cell bodies, sparsely distributed mainly in the molecular and granule layer, were also lightly immunostained, but the cell type could not be identified (Figure 8b).

At the rostral rhombencephalic tegmentum, numerous immunoreactive cell bodies were observed dorsally in the nucleus isthmi (NI) and some zones of the secondary gustatory/visceral nucleus (SGVN), as well as many fibers crossing the gustatory commissure (*cg*) (Figures 4j and 8c). In the ventral midline, the interpeduncular nucleus (Ip) also showed some immunoreactive cell bodies and a few immunoreactive fibers mainly in the dorsal neuropil (Figures 4i and 8d). Nrgn-like-ir cell bodies were also sparsely distributed in the superior reticular formation, the central gray (gr) and the raphe (r) (Figure 4j). Some Nrgn-like-ir fibers were seen in the secondary gustatory tract (*sgt*) and also crossing the midline through the rhombencephalic ventral commissure (*cven*) (Figures 4k and 8e). At this level, Nrgn-like positive fiber bundles appeared at the margin of the ventromedial and the ventrolateral tegmentum, likely the tectobulbaris rectus (*tbr*) and cruciatus (*tbc*) tracts (Figure 4i–j).

At the level of entrance of the trigeminal nerve (nV), many Nrgn-like positive cell bodies were observed in two groups: (1) a group located just dorsal to the sensory trigeminal nerve root entrance and ventral to the cerebellar eminentia granularis and (2) another group located near the ventrolateral border of the fourth ventricle and that likely corresponds with the principal sensory trigeminal nucleus (STN) (Figures 4k and 8e). Related to a small immunoreactive bundle coursing at the ventrolateral margin of the tegmentum (apparently continuous with the torobulbar tract described above), immunopositive fibers appear to course in the trigeminal area and to the lateral lemniscus (Figures 4k and 8e). Sparser Nrgn-like-ir fibers innervate the ventromedial tegmentum and cross in the rhombencephalic ventral commissure (Figures 4k and 8e).

At the level of the octaval nerve entrance, the medial octavolateral nucleus (MON) showed Nrgn-like-ir crest cells extending thick apical dendrites to the overlying cerebellar crest (CC), which is continuous with the molecular layer of the cerebellum (Figures 4l,m and 8f,g). Basal dendrites of these cells form a dense plexus within the nucleus among crest cell bodies (Figure 8g). A group of small Nrgn-like-ir cell bodies was also seen close to the lateral dendrite of the giant Mauthner cell (M) (Figures 4l and 8h). Caudally, some Nrgn-like-ir cell bodies were observed in the facial (LVII), glossopharyngeal (LIX) and vagal (LX) lobes, and a few in the commissural nucleus of Cajal (nC) (Figures 4 m–o and 8i,j). Most of the Nrgn-like-ir neurons of the LX were pear-shaped cells located in the cortex of the lobe and with conspicuous processes directed radially to the core region (Figure 8j). Vagal lobes appeared bilaterally related to positive fibers coursing in the commissural tract (arcuate fibers) (Figure 4n). Furthermore, compact Nrgn-like-ir fiber bundles arising from the facial and vagal lobes entered the ipsilateral *sgt* (Figure 8k). In the caudal rhombencephalon, immunoreactive cell bodies were observed in tegmental regions, both in the intermediate reticular formation and in the inferior olive (IO) (Figures 4l–n and 8i–m). At the transition with the spinal cord, numerous Nrgn-like-ir cell bodies and fibers were seen in the medial funicular nucleus (Figures 4o,p and 8m).

4 | DISCUSSION

4.1 | Neurogranin-like peptides in zebrafish

Our western blot results seem to confirm the expression of three neurogranin peptides in zebrafish, as predicted based on gene and transcript sequences. SDS–PAGE protein separation and western blot analysis showed three different bands of approximately 13, 20 and 37 kDa, which likely correspond to the three neurogranin peptides, Nrgna-60, Nrgna-92, and Nrgnb-188, predicted from zebrafish sequences. Two of these peptides (Nrgna-60 and Nrgna-92) would be translated from *nrgna*, while the third larger peptide Nrgnb-188 would be so from *nrgnb*. The molecular weights for these peptides deduced from the amino acid sequences are almost half (6.9, 10.6,

20.9 kDa) of those showed in the SDS–PAGE/western blot, but this apparent discrepancy has also been shown for rat neurogranin and neuromodulin (Baudier et al., 1991; Huang et al., 1993; Represa et al., 1990; Watson et al., 1990). We also ruled out the possibility that the three bands observed were the result of neurogranin dimerization and/or oligomerization, as this is prevented by using a reducing agent (Baudier et al., 1991; Wu et al., 2003). Interestingly, the other teleost included in the analysis, the gray mullet, also showed three bands of similar molecular weights to those in zebrafish.

Our protein sequence analysis showed that zebrafish Nrgna-60 and Nrgna-92 have a higher identity with rat neurogranin than Nrgnb-188. It has been shown that *nrgnb* is related to vascular development and hematopoiesis (Gómez et al., 2012; Wong et al., 2009), being also referred to as "sperm auto antigen 17" (spa17; Gómez et al., 2012). However, *nrgnb* shows much less identity with rat *spa17* (UniProtKB - Q9Z1K2-spa17) than with rat neurogranin (46.15% and 61.54%, respectively).

Analysis of the IQ domain among different species (Clayton et al., 2009; present results) showed a glycine substitution in teleosts, instead of the serine (Ser) present in cladistia and tetrapods (apart from *Xenopus*). The presence of this Ser in the bichir (*E. calabaricus*), a representative of the basal actinopterygii and sister lineage of all other ray-finned fish, suggests the derived character of the glycine substitution observed in teleosts. Phosphorylation of neurogranin by PKC has been shown to occur precisely in this serine located in the IQ domain (Ser36) in mammals (Gerendasy et al., 1994, 1995). Likely because of the functional role of this serine, it has been conserved in various species of mammals including prototherians, reptiles and birds (Baudier et al., 1989, 1991; Clayton et al., 2009; Deloulme et al., 1991; Gerendasy et al., 1994; Piosik et al., 1995; Watson et al., 1990; present results). Mammalian variant proteins in which Ser36 was substituted for other amino acids vary in their biochemical properties and failed to serve as a substrate for PKC phosphorylation (Gerendasy et al., 1995; Watson et al., 1996), not being the case for other proteins of the family (calpacitin proteins) (Slemmon et al., 1996). The glycine (Gly) substitution in teleosts could not only affect PKC phosphorylation but also its alpha-helical structure and affinity for calmodulin (Gerendasy et al., 1994). Thus, further biochemical studies will be necessary to determine how the Ser36 > Gly substitution in teleosts affects neurogranin structure and molecular interactions. Despite the Ser36 > Gly substitution, the teleostean IQ domain conserves the arginine in position 38, which seems to have an essential role in the IQ domain–calmodulin interaction (Kumar et al., 2013). This interaction is also possible because the IQ domain in zebrafish conserved most of the crucial amino acids involved in it (I33, F37, R38, H40, M41, R43, K44, K45, and K47; Kumar et al., 2013).

4.2 | Neurogranin immunohistochemistry

Our results indicate that Nrgn-like immunoreactivity is widely distributed in neurons of the brain and cells of sensory systems of the adult zebrafish. Based on cell morphologies and location, it seems that immunoreactivity in the brain is observed in neurons. The ependymoglia, the most abundant and easily identifiable macroglial cell type in zebrafish and other teleosts (Díaz-Regueira & Anadón, 1998), was always Nrgn-like negative. Although neurogranin expression in other glial cells cannot be ruled out without additional experiments, positive cells were lacking in the major white matter tracts where oligodendrocytes typically abound in teleosts (Díaz-Regueira & Anadón, 1998), which strongly suggests that these cells do not express this peptide in adult zebrafish. Since neurogranins are present in sensory organs and most brain systems (i.e., sensory, motor, integrative), they must have a basic function, not determined by cell type or structure. This basic role is compatible with previous studies showing that neurogranin may play roles in the regulation of synaptic plasticity (Li et al., 2020; Zhong et al., 2011; Zhong & Gerges, 2020), likely by favoring LTP over long-term depression (Zhong & Gerges, 2020). The exact mechanism by which this regulation is achieved is still under investigation (Li et al., 2020; Zhong et al., 2011; Zhong & Gerges, 2020). We observe that there are three Nrgn-like peptides in zebrafish and mullet, which could mediate different functions in specific cell types and brain regions through interaction with particular signaling pathways. Further studies will be needed to clarify this point, analyzing the expression of each specific peptide.

Although very broadly distributed, we do observe that neurogranins show expression in specific cell types in the brain, as we will discuss in the following paragraphs.

4.2.1 | Distribution of Nrgn-like immunoreactivity in sensory organs

Neurogranin immunoreactivity was observed in cells of sensory structures such as the gustatory, the olfactory and the visual systems of the adult zebrafish. In our literature searchs, we found no mention of neurogranin expression in these sensory organs. In zebrafish, barbels with taste buds develop in the juvenile stage, at least 1 month after the appearance of the other taste buds in the body surface and oropharyngeal cavity (Hansen et al., 2002). The distribution of neurogranin immunofluorescence observed in barbel taste buds suggests that at least the cells with a single large microvillus express neurogranin. These cells correspond with the light taste bud cells described based on electron microscopy (Hansen et al., 2002).

In the olfactory organ, bipolar neurons with perikarya in the middle of the sensory epithelium are the most common Nrgn-like positive cells, but the subtype(s) of sensory neuron (ciliary, microvillous, crypt: see Gayoso et al., 2011, 2012) was not assessed.

In the retina of adult zebrafish, we observed Nrgn-like immunoreactivity mainly in bipolar cells but also some photoreceptors, amacrine and ganglion cells. Different types of bipolar cells were described based on morphology, connections and neurochemical features in zebrafish and other cyprinids (Connaughton et al., 2004; Li et al., 2012; Marc & Cameron, 2001; Sherry & Yazulla, 1993). PKC, which may use neurogranin as substrate (Baudier et al., 1991), was described by immunocytochemical techniques in bipolar cells of the vertebrate retina,

including cyprinids (Caminos et al., 2000; Yazulla & Studholme, 2001), which are likely to correspond to ON-bipolar cells (Haug et al., 2019). Based on shape and location, the PKC-ir bipolar cells described by these authors resemble the Nrgn-like-ir bipolar cells described here. Whereas PKC immunoreactivity intensely labels bipolar cell terminals in three sublaminae of the IPL (Nevin et al., 2008), only weak immunoreactivity against neurogranin was observed in the IPL, suggesting it has a postsynaptic location in these bipolar cells.

4.2.2 | Distribution of Nrgn-like immunoreactivity in the zebrafish brain

Studies on the general distribution of neurogranin in the brain are limited to a few in mammals (Represa et al., 1990), lacking data in non-mammalian species. Here, we report that Nrgn-like immunoreactivity is expressed in numerous brain regions of zebrafish, extending from the olfactory bulb to the hindbrain. The pattern observed presents numerous differences with that reported in mammals (discussed below) and, as far as we are aware, represents the first description in a nonmammalian vertebrate.

In the olfactory bulb, occasional immunoreactive cell bodies (likely periglomerular cells) were observed among positive fibers of the glomerular layer. However, most Nrgn-like expression in the bulbs appears in axon terminals of a part of the glomeruli, suggesting a presynaptic distribution of this protein. The almost absence of positive fibers in the olfactory tracts and the main pallial olfactory target (Dp; Gayoso et al., 2011, 2012; Yáñez et al., 2021) suggests that secondary olfactory projections do not use neurogranin. Neurogranin expression has been described in a subpopulation of GABAergic granule cells of the main and accessory olfactory bulbs of the mouse but not in mitral cells (Gribaudo et al., 2009). GABA expression has also been demonstrated in granule cells of the olfactory bulb in zebrafish (Kim et al., 2004; Mueller & Guo, 2009), in which we also observe Nrgn-like expression.

Our results showed that Nrgn-like-ir cell bodies are present in most areas of the pallium of adult zebrafish, although with slight differences in their intensity of immunoreaction. Strong expression of the *nrgn* gene in the dorsal telencephalon was also observed in 6-day-old larvae (Zada et al., 2014). In this regard, expression in zebrafish is similar to the cortex of mammals (neocortex and hippocampus), which expresses neurogranin in numerous principal neurons (Represa et al., 1990; Singec et al., 2004). Neurogranin has been related to synaptic plasticity and learning in higher brain regions (Díez-Guerra, 2010; Pak et al., 2000; Zhong et al., 2009, 2015), but to date no functional studies have been performed in zebrafish. The dorsal (Dd) and some subdivisions of the medial area of D (Dm) showed the highest intensity of immunoreaction at pre- and postcommissural levels, as some cells of the central area (Dc). Most authors consider areas of the actinopterygian pallium homologous to the mammalian hippocampus (Dld), neocortex (Dc), and pallial amygdala (Dm), although it is still a matter of debate (Folgueira et al., 2004b, 2012; Ganz et al., 2014; Nieuwenhuys, 2009; Northcutt, 2008, 2011; Porter & Mueller, 2020; Wullimann & Mueller, 2004; N. Yamamoto et al., 2007; K. Yamamoto et al., 2017; Yáñez et al., 2021). Interestingly, Dm and Dl are involved in different learning tasks in carps (Portavella et al., 2002, 2004), which suggests that the Nrgn-like abundance in these regions may be related to adaptation in learning circuits. On the other hand, the olfactory pallium (Dp) in zebrafish is devoid of Nrgn-like-ir cells and fibers, which is unlike the abundance in the pyriform cortex, the mammalian homologous olfactory region (Álvarez-Bolado et al., 1996; Gribaudo et al., 2009; Represa et al., 1990). Unlike in mammals, where immunoreactivity is located in dendrites and somas (Singec et al., 2004), bundles of Nrgn-like positive fibers coming from Dd and other D areas coursed in the lateral and the medial telencephalic tracts, and can be followed caudally to tuberculohypothalamic levels. In the mammalian cortex, neurogranin is considered part of the postsynaptic molecular networks (Zhong et al., 2015). In teleosts, it is possible that neurogranins may act both in postsynaptic and presynaptic processes, as reported in the mammalian spinal cord (Houben et al., 2000). To elucidate the possible presynaptic or postsynaptic roles of each of the zebrafish neurogranins in different circuits, it would be necessary to analyze separately their brain distribution, which was not possible with the method used here.

In the zebrafish subpallium, Nrgn-like immunoreactivity was observed in some cell bodies of several subdivisions at precommissural (Vv, Vd, Vc) and commissural (Vs) levels. Following the proposed homologies between the tetrapod subpallium and the noneverted ventral area of the telencephalon of teleosts (Folgueira et al., 2004a; Ganz et al., 2012; Northcutt, 1995; Rink & Wullimann, 2004), Nrgn-ir cells are mainly distributed in the striatum and pallidum homologs. These regions are part of the basal ganglia and show neurogranin expression in the rat (Represa et al., 1990). Neurogranin is involved in the regulation of sensory-motor responses via cortico-striatal circuits (Sullivan et al., 2019), but these circuits have not been analyzed in detail in zebrafish.

The hypothalamus and diencephalic regions (prethalamus, thalamus, posterior tubercle and pretectum) have some nuclei with Nrgn-like-ir cells. Noteworthy, we observed a number of neurogranin positive cells in the nucleus rostrolateralis, whose neurochemistry and organization have been poorly characterized. This nucleus is considered an epithalamic visual center present in a discrete number of actinopterygians, including zebrafish (Butler & Saidel, 2003; Saidel, 2013; Saidel & Butler, 1997). Nrgn-like immunoreactivity is also expressed intensely in some thalamic, pretectal and preglomerular nuclei that are considered relay centers between major sensory systems and the pallium or other major systems (Yáñez et al., 2018). However, the rat diencephalon shows very poor neurogranin immunolabeling (Represa et al., 1990), representing a major difference with results in zebrafish.

It is noteworthy the presence of numerous Nrgn-like-ir neurons with CSF-contacting morphology, in the hypothalamic paraventricular organ and the posterior recess organ (Hc of Wullimann et al., 1996; posterior part of the paraventricular organ of Kaslin & Panula, 2001). These circumventricular organs also show numerous monoaminergic CSF-contacting neurons (Kaslin & Panula, 2001; Xavier et al., 2017; K. Yamamoto et al., 2010). We observed an Nrgn-positive mat of fibers associated with these organs that strongly resemble the

monoaminergic tracts reported with histofluorescence, which relate all the hypothalamic circumventricular organs of teleosts (see Gómez-Segade et al., 1989). Immunochemical studies show CSF-contacting neurons of hypothalamic circumventricular organs of teleosts having perikarya with a simple bipolar appearance, but transmission electron microscopy reveals that the apical region of the cell dendrites, including the supraventricular part, receives a surprising number of synaptic contacts, forming together a complex intraventricular mat of processes (Gómez-Segade et al., 1989). This may explain the Nrgn-like expression in dendrites of these cells, which are actually postsynaptic to a number of thin intraventricular axons.

The OT is a multisensory integrative midbrain center in zebrafish and other nonmammalian vertebrates, involved in visually guided behavior and being homologous to the mammalian superior colliculus (Meek & Nieuwenhuys, 1998). In zebrafish, Nrgn-like-ir perikarya are abundant in different tectal layers, mostly in the SPV, but also in the SAC, SGC and SFGS. This is in contrast with the poor expression of neurogranin in the rodent's superior colliculus (Represa et al., 1990). These differences may stress that the retinotectal pathway is less important than the retinogeniculate pathway in the visual behavior of these rodents, that is, the shift toward the visual telencephalon for different tasks performed by the OT in fishes (Knudsen, 2020). The apical dendrites from SGC and SFGS neurons can occasionally extend to the SM of the OT, which is part of a cerebellum-like circuit that receives parallel fibers from the TLo (Bell et al., 2008; Folgueira et al., 2020). This tectal parallel fiber system is Nrgn-like negative, as it is the case of parallel fibers in the cerebellum (see below). In the midbrain, too, many Nrgn-like-ir cell bodies and fibers were located in the TS, the homologous of the mammalian inferior colliculus. It is involved in processing mechanosensory information (octaval, lateral line and trigeminal) in nonelectroreceptive teleosts (McCormick & Hernández, 1996; N. Yamamoto et al., 2010). In the rat, the inferior colliculus also shows some neurogranin expression (Represa et al., 1990).

A notable difference between our results with neurogranin and those in mammals (Represa et al., 1990) is the presence of this protein in numerous hindbrain structures of zebrafish (interpeduncular nucleus, NI, cerebellum and cerebellum-like structures, gustatory/visceral sensory nuclei, etc.). This is also supported by in situ hybridization studies that reveal abundant *nrgn* gene expression in the hindbrain of 6-day-old zebrafish larvae (Zada et al., 2014). In the interpeduncular nucleus (Ip), neurogranin expression was observed in cell bodies and fibers, mainly in the dorsal neuropil. The high proportion of Nrgn-like positive structures in the dorsal plexus is related to the asymmetrical innervation from the habenulae and probably with the plasticity of fear responses and other behaviors (Agetsuma et al., 2010; Cherng et al., 2020). No expression of neurogranin has been reported in the Ip of mammals (Represa et al., 1990), which indicates differential adaptation roles.

In teleosts, the cerebellum consists of three main regions: the cerebellar valvula, the corpus cerebelli and the vestibulolateralis lobe (Meek & Nieuwenhuys, 1998; Nieuwenhuys, 1967). In the adult zebrafish, Nrgn-like immunoreactivity was observed mainly in Purkinje cells, although their dendritic arbors of these cells were only evident in the medial division of the cerebellar valvula. In this cerebellar region, Purkinje cell dendrites extend in the molecular layer in a pattern similar to that in mammals (Miyamura & Nakayasu, 2001). Zebrafish Purkinje cells use GABA as neurotransmitter and express *parvalbumin7* and zebrin II (Bae et al., 2009; Delgado & Schmachtenberg, 2008; Lannoo et al., 1991b). In teleosts, most Purkinje cells project onto neighbor efferent neurons, the eurydendroid cells, which are glutamatergic and calretinin positive (Bae et al., 2009; Castro et al., 2006b; Ikenaga et al., 2005, 2006a; Murakami & Morita, 1987). Without labeling experiments with markers of eurydendroid cells and neurogranin, we cannot rule out the possibility that some eurydendroid cells also express neurogranin. Results in the zebrafish cerebellum are similar to adult songbirds, in which high neurogranin expression was also described in Purkinje cells (Clayton et al., 2009). In the adult mammalian cerebellum, neurogranin is strongly expressed by inhibitory cells, mostly in a subpopulation of Golgi cells in rodents and, during development, in some bands of Purkinje cells (Larouche et al., 2006; Simat et al., 2007; White & Sillitoe, 2013). In monkeys, neurogranin is also expressed in the excitatory brush cells (Singec et al., 2004). With regard to the major precerebellar centers of zebrafish, the IO contains Nrgn-like-ir neurons, while the NLV shows Nrgn-like immunoreactivity in the characteristic cup-shaped afferents embracing the neurons of the nucleus (Yang et al., 2004). These results suggest that neurogranins are implicated presynaptically in the NLV and postsynaptically in Purkinje cells, pretectum, and IO.

Prominent Nrgn-like immunoreactivity is also observed in the characteristic crest cells of the MON, which are the principal cells of this nucleus, which receives primary mechanosensory fibers from the lateral line nerves (see Fame et al., 2006; McCormick & Hernández, 1996; Meek & Nieuwenhuys, 1998). Crest cells are Purkinje-like complex neurons with apical dendrites that extend in the CC and synapse with parallel fibers arising from the cerebellar eminentia granularis (Díaz & Anadón, 1989; Meredith, 1984). Cerebellar Purkinje cells and MON crest cells also share expression of the GABAergic markers genes (*gad1* and *gad2*), *parvalbumin7* (Bae et al., 2009) and, some of them, also the Nrgn positivity in apical dendrites.

The primary and secondary centers of the gustatory and general visceral sensory system are highly specialized in some teleosts, as cyprinids and silurids (Finger, 2009; Ikenaga et al., 2009; Yáñez et al., 2017). We found that Nrgn-like-ir cell bodies were abundant in the facial, glossopharyngeal and vagal lobes (primary centers), the secondary gustatory/visceral centers (SGVN), and also in the so-called TGN proper by us (Yáñez et al., 2017). Note that this TGN nucleus does not correspond to the TGN of Wullimann et al. (1996), which does not receive TGN fibers at all (see Yáñez et al., 2017). If the TGN proper is the homolog of the big carp TGN, however, needs to be assessed with other molecular markers. In the goldfish vagal lobe, NMDA glutamate receptors facilitate short-term amplification of bursts of inputs coming from the vagal nerve (Smeraski et al., 1999), and calcium-binding proteins and channels are abundant (Ikenaga et al., 2006b). The abundance of Nrgn-like immunoreactivity in taste centers in zebrafish suggests that neurogranin may be implicated in plasticity and adaptation in taste

processing. These results in zebrafish are in contrast with results in the rat indicating that the hindbrain mostly lacks neurogranin expression (Represa et al., 1990).

5 | CONCLUSIONS

Database analysis indicates the presence of three neurogranin peptides in zebrafish with a conserved IQ domain that differs from that in mammals and birds in a serine to glycine substitution in position 36, which is phosphorylated by PKC. Thus comparison with Nrgn in amniotes suggests possible differences in the regulation by PKC between actinopterygians and land vertebrates. Western blots of protein extracts from zebrafish brain using a specific anti-neurogranin antiserum revealed three protein bands, in good agreement with predictions from database analysis. Since the antibody used binds to the three neurogranin peptides, immunohistochemical results do not allow to differentiate the distribution of the individual peptides in the brain. In our immunohistochemical analysis, we have studied the brain and some sensory organs (barbel taste buds, neuromasts, olfactory rosette and retina) revealing positive cell bodies in all these structures. Positive cells in the barbel taste buds appear to be sensory taste cells, while in the other places examined positivity was observed in neurons, and the expression was cell-type specific. In the retina, the most conspicuous positive cells are bipolar neurons, probably rod bipolar cells. In the brain, we observed immunopositive neuronal populations in all major brain regions (telencephalon, preoptic area, hypothalamus, diencephalon, mesencephalon and rhombencephalon, including the cerebellum), a more extended distribution than that reported in mammals. Interestingly, in several brain regions the dendrites, cell bodies and axon terminal of neurons were immunopositive. This suggests that neurogranins may play both presynaptic and postsynaptic roles in zebrafish. Most Nrgn-like immunoreactive neurons were found either in primary sensory centers (viscerosensory column, MON) or in highly integrative centers (such as the pallium and subpallium, OT, and cerebellum). This may suggest that neurogranins are mainly expressed in centers with complex synaptic circuitry in zebrafish. However, there are exceptions, as some apparently simple neuronal populations, as the positive CSF-contacting cells associated with the hypothalamic recesses, exhibited high Nrgn-like immunoreactivity. Together, these results reveal some important differences with the patterns reported in mammals, suggesting divergent evolution from an early common ancestor.

ACKNOWLEDGMENTS

AA-G was funded by a Predoctoral Fellowship from Xunta de Galicia (grant number ED481A-2019/003).

CONFLICT OF INTEREST

The authors declare no conflict of interest. All authors had access to all the data in the study and take responsibility for the integrity of the data and the accuracy of the data analysis.

AUTHOR CONTRIBUTIONS

Study concept and design: AA-G, MF, and JY. Database sequence retrieval and sequence comparison: AA-G and MF. Western blot data: AA-G and AC. Immunohistochemistry data: AA-G and JY. Analysis and interpretation of data: AA-G, JY, RA and MF. Drafting of the manuscript and final version: AA-G, JY, RA and MF.

PEER REVIEW

The peer review history for this article is available at https://publons.com/publon/10.1002/cne.25297.

DATA AVAILABILITY STATEMENT

The data that support the findings of this study are available from the corresponding author upon reasonable request.

ORCID

Anabel Alba-González https://orcid.org/0000-0003-1627-3006
Mónica Folgueira https://orcid.org/0000-0003-2927-7516
Ramón Anadón https://orcid.org/0000-0003-3260-1209
Julián Yáñez https://orcid.org/0000-0002-4559-8398

REFERENCES

Agetsuma, M., Aizawa, H., Aoki, T., Nakayama, R., Takahoko, M., Goto, M., Sassa, T., Amo, R., Shiraki, T., Kawakami, K., Hosoya, T., Higashijima, S. I., & Okamoto, H. (2010). The habenula is crucial for experience-dependent modification of fear responses in zebrafish. *Nature Neuroscience*, *13*, 1354–1356. https://doi.org/10.1038/nn.2654

Aleström, P., D'Angelo, L., Midtlyng, P. J., Schorderet, D. F., Schulte-Merker, S., Sohm, F., & Warner, S. (2020). Zebrafish: Housing and husbandry recommendations. *Laboratory Animals*, *54*, 213–224. https://doi.org/10.1177/0023677219869037

Álvarez-Bolado, G., Rodríguez-Sánchez, P., Tejero-Diez, P., Fairén, A., & Diez-Guerra, F. J. (1996). Neurogranin in the development of the rat telencephalon. *Neuroscience*, *73*, 565–580. https://doi.org/10.1016/0306-4522(96)00061-9

Bae, Y. K., Kani, S., Shimizu, T., Tanabe, K., Nojima, H., Kimura, Y., Higashijima, S., & Hibi, M. (2009). Anatomy of zebrafish cerebellum and screen for mutations affecting its development. *Developmental Biology*,*330*, 406–426. https://doi.org/10.1016/j.ydbio.2009.04.013

Barreiro-Iglesias, A., Mysiak, K. S., Adrio, F., Rodicio, M. C., Becker, C. G., Becker, T., & Anadón, R. (2013). Distribution of glycinergic neurons in the brain of glycine transporter-2 transgenic Tg(glyt2:Gfp) adult zebrafish: Relationship to brain-spinal descending systems. *The Journal of Comparative Neurology*, *521*, 389–425. https://doi.org/10.1002/cne.23179

Barros, T. P., Alderton, W. K., Reynolds, H. M., Roach, A. G., & Berghmans, S. (2008). Zebrafish: An emerging technology for in vivo pharmacological assessment to identify potential safety liabilities in early drug discovery. *British Journal of Pharmacology*, *154*, 1400–1413. https://doi.org/10.1038/bjp.2008.249

Baudier, J., Bronnerll, C., Kligman, D., & Cole, D. R. (1989). Protein kinase C substrates from bovine brain. *The Journal of Biological Chemistry*, *264*, 1824–1828. https://doi.org/10.1016/S0021-9258(18)94262-6

Baudier, J., Deloulme, J. C., Van Dorsselaer, A., Black, D., & Matthes, H. W. D. (1991). Purification and characterization of a brain-specific protein kinase C substrate, Neurogranin (p 17): Identification of a consensus amino acid sequence between neurogranin and neuromodulin (GAP-43) that corresponds to the protein kinase C phosphorylation site and the calmodulin-binding domain. *The Journal of Biological Medicine*, *266*, 229–237. https://doi.org/10.1016/S0021-9258(18)52425-X

Bell, C. C., Han, V., & Sawtell, N. B. (2008). Cerebellum-like structures and their implications for cerebellar function. *Annual Review of Neuroscience*, *31*, 1–21. https://doi.org/10.1146/annurev.neuro.30.051606.094225

Butler, A. B., & Saidel, W. M. (2003). Clustered phylogenetic distribution of nucleus rostrolateralis among ray-finned fishes. *Brain, Behavior and Evolution*, *62*, 152–168. https://doi.org/10.1159/000072724

Caminos, E., Velasco, A., Jarrín, M., Lillo, C., Jimeno, D., Aijón, J., Lara, J. M., & Lara, J. M. (2000). A comparative study of protein kinase C-like immunoreactive cells in the retina. *Brain, Behavior and Evolution*, *56*, 330–339. https://doi.org/10.1159/000047217

Cassar, S., Adatto, I., Freeman, J. L., Gamse, J. T., Iturria, I., Lawrence, C., Muriana, A., Peterson, R. T., Van Cruchten, S., & Zon, L. I. (2020). Use of zebrafish in drug discovery toxicology. *Chemical Research in Toxicology*, *33*, 95–118. https://doi.org/10.1021/acs.chemrestox.9b00335

Castro, A., Becerra, M., Manso, M. J., & Anadón, R. (2006a). Calretinin immunoreactivity in the brain of the zebrafish, *Danio rerio*: Distribution and comparison with some neuropeptides and neurotransmitter-synthesizing enzymes. I. Olfactory organ and forebrain. *The Journal of Comparative Neurology*, *494*, 435–459. https://doi.org/10.1002/cne.20782

Castro, A., Becerra, M., Manso, M. J., & Anadón, R. (2006b). Calretinin immunoreactivity in the brain of the zebrafish, *Danio rerio*: Distribution and comparison with some neuropeptides and neurotransmitter-synthesizing enzymes. II. Midbrain, hindbrain, and rostral spinal cord. *The Journal of Comparative Neurology*, *494*, 792–814. https://doi.org/10.1002/cne.20843

Castro, A., Becerra, M., Manso, M. J., Tello, J., Sherwood, N. M., & Anadón, R. (2009). Distribution of growth hormone-releasing hormone-like peptide: Immunoreactivity in the central nervous system of the adult zebrafish (*Danio rerio*). *The Journal of Comparative Neurology*, *513*, 685–701. https://doi.org/10.1002/cne.21977

Cherng, B., Islam, T., Torigoe, M., Tsuboi, T., & Okamoto, H. (2020). The dorsal lateral habenula-interpeduncular nucleus pathway is essential for left-right-dependent decision making in zebrafish. *Cell Reports*, *32*, 108143. https://doi.org/10.1016/j.celrep.2020.108143

Clayton, D. F., George, J. M., Mello, C. V., & Siepka, S. M. (2009). Conservation and expression of iq-domain-containing calpacitin gene products (neuromodulin/GAP-43, neurogranin/RC3) in the adult and developing oscine song control system. *Developmental Neurobiology*, *69*, 124–140. https://doi.org/10.1002/dneu.20686

Coggins, P. J., Mclean, K., & Zwiers, H. (1993). Neurogranin, a B-50/GAP-43-immunoreactive C-kinase substrate (BICKS), is ADP-ribosylated. *Federation of European Biochemical Societies*, *335*, 109–113. https://doi.org/10.1016/0014-5793(93)80450-9

Connaughton, V. P., Graham, D., & Nelson, R. (2004). Identification and morphological classification of horizontal, bipolar, and amacrine cells within the zebrafish retina. *The Journal of Comparative Neurology*, *477*, 371–385. https://doi.org/10.1002/cne.20261

Delgado, L., & Schmachtenberg, O. (2008). Immunohistochemical localization of GABA; GAD65, and the receptor subunits $GABA_{A\alpha1}$ and $GABA_{B1}$ in the zebrafish cerebellum. *Cerebellum (London, England)*, *7*, 444–450. https://doi.org/10.1007/s12311-008-0047-7

Deloulme, J., Sensenbrenner, M., & Baudier, J. (1991). A rapid purification method for neurogranin, a brain specific calmodulin-binding protein kinase C substrate. *Federation of European Biochemical Societies*, *282*, 183–188. https://doi.org/10.1016/0014-5793(91)80473-g

Díaz, S. M., & Anadón, R. (1989). Central projections of the lateral line nerves of *Chelon labrosus* (teleosts, order Perciformes). *Journal fur Hirnforschung*, *30*, 339–347.

Díaz-Regueira, S. M., & Anadón, R. (1998). The macroglia of teleosts: Characterization, distribution and development. In B. Castellano, B. González, & M. Nieto-Sampedro (Eds.), *understanding glial cells* (pp. 19–46). Springer, Boston, MA. https://doi.org/10.1007/978-1-4615-5737-1_2

Díez-Guerra, F. J. (2010). Neurogranin, a link between calcium/calmodulin and protein kinase C signaling in synaptic plasticity. *IUBMB Life*, *62*, 597–606. https://doi.org/10.1002/iub.357

Domínguez-González, I., Vázquez-Cuesta, S. N., Algaba, A., & Díez-Guerra, F. J. (2007). Neurogranin binds to phosphatidic acid and associates to cellular membranes. *Biochemical Journal*, *404*, 31–43. https://doi.org/10.1042/BJ20061483

Eisen, J. S. (1991). Developmental neurobiology of the zebrafish. *The Journal of Neuroscience*, *11*, 311–317. https://doi.org/10.1523/JNEUROSCI.11-02-00311.1991

Fame, R. M., Brajon, C., & Ghysen, A. (2006). Second-order projection from the posterior lateral line in the early zebrafish brain. *Neural Development*, *1*(4), 4. https://doi.org/10.1186/1749-8104-1-4

Finger, T. E. (2009). Evolution of gustatory reflex systems in the brainstems of fishes. *Integrative Zoology*, *4*, 53–63. https://doi.org/10.1111/j.1749-4877.2008.00135.x

Folgueira, M., Anadón, R., & Yáñez, J. (2004a). An experimental study of the connections of the telencephalon in the rainbow trout (*Oncorhynchus mykiss*). I: Olfactory bulb and ventral area. *The Journal of Comparative Neurology*, *480*, 180–203. https://doi.org/10.1002/cne.20340

Folgueira, M., Anadón, R., & Yáñez, J. (2004b). Experimental study of the connections of the telencephalon in the rainbow trout (*Oncorhynchus mykiss*). II: Dorsal area and preoptic region. *The Journal of Comparative Neurology*, *480*, 204–233. https://doi.org/10.1002/cne.20341

Folgueira, M., Bayley, P., Navratilova, P., Becker, T. S., Wilson, S. W., & Clarke, J. D. W. (2012). Morphogenesis underlying the development of the everted teleost telencephalon. *Neural Development*, *7*(32). https://doi.org/10.1186/1749-8104-7-32

Folgueira, M., Riva-Mendoza, S., Ferreño-Galmán, N., Castro, A., Bianco, I. H., Anadón, R., & Yáñez, J. (2020). Anatomy and connectivity of the torus longitudinalis of the adult zebrafish. *Frontiers in Neural Circuits*, *14*, 8. https://doi.org/10.3389/fncir.2020.00008

Fulwiler, C., & Gilbert, W. (1991). Zebrafish embryology and neural development. *Current Opinion in Cell Biology*, *3*, 988–991. https://doi.org/10.1016/0955-0674(91)90118-I

Ganz, J., Kaslin, J., Freudenreich, D., Machate, A., Geffarth, M., & Brand, M. (2012). Subdivisions of the adult zebrafish subpallium by molecular marker analysis. *The Journal of Comparative Neurology*, *520*, 633–655. https://doi.org/10.1002/cne.22757

Ganz, J., Kroehne, V., Freudenreich, D., Machate, A., Geffarth, M., Braasch, I., Kaslin, J., & Brand, M. (2014). Subdivisions of the adult zebrafish pallium based on molecular marker analysis. *F1000Research*, *3*, 308. https://doi.org/10.12688/f1000research.5595.1

Gayoso, J., Castro, A., Anadón, R., & Manso, M. J. (2011). Differential bulbar and extrabulbar projections of diverse olfactory receptor neuron populations in the adult zebrafish (*Danio rerio*). *The Journal of Comparative Neurology*, *519*, 247–276. https://doi.org/10.1002/cne.22518

Gayoso, J., Castro, A., Anadón, R., & Manso, M. J. (2012). Crypt cells of the zebrafish *Danio rerio* mainly project to the dorsomedial glomerular field of the olfactory bulb. *Chemical Senses*, *37*, 357–369. https://doi.org/10.1093/chemse/bjr109

Gerendasy, D. D., & Sutcliffe, J. G. (1997). Molecular neurobiology RC3/neurogranin, a postsynaptic calpacitin for setting the response threshold to calcium influxes. *Molecular Neurobiology*, *15*, 131–163. https://doi.org/10.1007/bf02740632

Gerendasy, D. D., Herron, S. R., Jennings, P., & Sutcliffe, J. G. (1995). Calmodulin stabilizes an amphiphilic α-helix within RC3/neurogranin and GAP-43/neuromodulin only when Ca^{2+} is absent. *The Journal of Biological Chemistry*, *270*, 6741–6750. https://doi.org/10.1074/jbc.270.12.6741

Gerendasy, D. D., Herron, S. R., Watson, J. B., & Sutcliffe, J. G. (1994). Mutational and biophysical studies regulates calmodulin availability. *The Journal of Biological Chemistry*, *269*, 22420–22426. https://doi.org/10.1016/S0021-9258(17)31806-9

Gómez, G., Lee, J. H., Veldman, M. B., Lu, J., Xiao, X., & Lin, S. (2012). Identification of vascular and hematopoietic genes downstream of *etsrp* by deep

sequencing in zebrafish. *PloS One*, *7*(3), e31658. https://doi.org/10.1371/journal.pone.0031658

Gómez-Segade, P., Anadón, R., & Gómez-Segade, L. (1989). Monoaminergic systems in the hypothalamus of the acanthopterygian *Chelon labrosus* (Risso, 1826), with special reference to the organon vasculosum hypothalami. *Acta Zoologica*, *70*(1), 1–11. https://doi.org/10.1111/j.1463-6395.1989.tb01047.x

Gribaudo, S., Bovetti, S., Garzotto, D., Fasolo, A., & De Marchis, S. (2009). Expression and localization of the calmodulin-binding protein neurogranin in the adult mouse olfactory bulb. *The Journal of Comparative Neurology*, *517*, 683–694. https://doi.org/10.1002/cne.22177

Hansen, A., Reutter, K., & Zeiske, E. (2002). Taste bud development in the zebrafish, *Danio rerio*. *Developmental Dynamics*, *223*, 483–496. https://doi.org/10.1002/dvdy.10074

Haug, M. F., Berger, M., Gesemann, M., & Neuhauss, S. C. F. (2019). Differential expression of PKCα and -β in the zebrafish retina. *Histochemistry and Cell Biology*, *151*, 521–530. https://doi.org/10.1007/s00418-018-1764-8

Houben, M. P., Lankhorst, A. J., van Dalen, J. J., Veldman, H., Joosten, E. A., Hamers, F. P., Gispen, W. H., & Schrama, L. H. (2000). Pre- and postsynaptic localization of RC3/neurogranin in the adult rat spinal cord: An immunohistochemical study. *Journal of Neuroscience Research*, *59*, 750–759. https://doi.org/10.1002/(sici)1097-4547(20000315)59:6%3C750::aid-jnr7%3E3.0.co;2-b

Huang, K. P., Huang, F. L., & Chen, H. C. (1993). Characterization of a 7.5-kDa protein kinase C substrate (RC3 Protein, Neurogranin) from rat brain. *Archives of Biochemistry and Biophysics*, *305*, 570–580. https://doi.org/10.1006/abbi.1993.1463

Ikenaga, T., Yoshida, M., & Uematsu, K. (2005). Morphology and immunohistochemistry of efferent neurons of the goldfish corpus cerebelli. *The Journal of Comparative Neurology*, *487*, 300–311. https://doi.org/10.1002/cne.20553

Ikenaga, T., Yoshida, M., & Uematsu, K. (2006a). Cerebellar efferent neurons in teleost fish. *The Cerebellum*, *5*, 268–274. https://doi.org/10.1080/14734220600930588

Ikenaga, T., Huesa, G., & Finger, T. E. (2006b). Co-occurrence of calcium-binding proteins and calcium-permeable glutamate receptors in the primary gustatory nucleus of goldfish. *The Journal of Comparative Neurology*, *499*, 90–105. https://doi.org/10.1002/cne.21079

Ikenaga, T., Ogura, T., & Finger, T. E. (2009). Vagal gustatory reflex circuits for intraoral food sorting behavior in the goldfish: Cellular organization and neurotransmitters. *The Journal of Comparative Neurology*, *516*, 213–225. https://doi.org/10.1002/cne.22097

Karousis, E. D., & Mühlemann, O. (2019). Nonsense-mediated mRNA decay begins where translation ends. *Cold Spring Harbor Perspectives in Biology*, *11*(2). https://doi.org/10.1101/cshperspect.a032862

Kaslin, J., & Panula, P. (2001). Comparative anatomy of the histaminergic and other aminergic systems in zebrafish (*Danio rerio*). *The Journal of Comparative Neurology*, *440*, 342–377. https://doi.org/10.1002/cne.1390

Kim, Y. J., Nam, R. H., Yoo, Y. M., & Lee, C. J. (2004). Identification and functional evidence of GABAergic neurons in parts of the brain of adult zebrafish (*Danio rerio*). *Neuroscience Letters*, *335*, 29–32. https://doi.org/10.1016/j.neulet.2003.10.024

Knudsen, E. I. (2020). Evolution of neural processing for visual perception in vertebrates. *The Journal of Comparative Neurology*, *528*, 2888–2901. https://doi.org/10.1002/cne.24871

Koob, A. O., Shaked, G. M., Bender, A., Bisquertt, A., Rockenstein, E., & Masliah, E. (2014). Neurogranin binds α-synuclein in the human superior temporal cortex and interaction is decreased in Parkinson's disease. *Brain Research*, *1591*, 102–110. https://doi.org/10.1016/j.brainres.2014.10.013

Kumar, V., Chichili, V. P. R., Zhong, L., Tang, X., Velazquez-Campoy, A., Sheu, F. S., Seetharaman, J., Gerges, N. Z., & Sivaraman, J. (2013). Structural basis for the interaction of unstructured neuron specific substrates neuromodulin and neurogranin with calmodulin. *Scientific Reports*, *3*(1392). https://doi.org/10.1038/srep01392

Lamas, I., Anadón, R., & Díaz-Regueira, S. (2007). Carnosine-like immunoreactivity in neurons of the brain of an advanced teleost, the gray mullet (*Chelon labrosus*, Risso). *Brain Research*, *1149*, 87–100. https://doi.org/10.1016/j.brainres.2007.02.070

Lannoo, M. J., Brochu, G., Maler, L., & Hawkes, R. (1991a). Zebrin II immunoreactivity in the rat and in the weakly electric teleost *Eigenmannia* (gymnotiformes) reveals three modes of Purkinje cell development. *The Journal of Comparative Neurology*, *310*, 215–233. https://doi.org/10.1002/cne.903100207

Lannoo, M. J., Ross, L., Maler, L., & Hawkes, R. (1991b). Development of the cerebellum and its extracerebellar Purkinje cell projection in teleost fishes as determined by zebrin II immunocytochemistry. *Progress in Neurobiology*, *37*, 329–363. https://doi.org/10.1016/0301-0082(91)90022-S

Larouche, M., Che, P. M., & Hawkes, R. (2006). Neurogranin expression identifies a novel array of Purkinje cell parasagittal stripes during mouse cerebellar development. *The Journal of Comparative Neurology*, *494*, 215-227. https://doi.org/10.1002/cne.20791

Laufer, M., & Vanegas, H. (1974). The optic tectum of a perciform teleost II. Fine structure. *The Journal of Comparative Neurology*, *154*, 61–96. https://doi.org/10.1002/cne.901540105

Li, L., Lai, M., Cole, S., Le, Novère N., & Edelstein, S. J. (2020). Neurogranin stimulates Ca^{2+}/calmodulin-dependent kinase II by suppressing calcineurin activity at specific calcium spike frequencies. *PLoS Comput Biol.*, *16*(2), e1006991. https://doi.org/10.1371/journal.pcbi.1006991

Li, Y. N., Tsujimura, T., Kawamura, S., & Dowling, J. E. (2012). Bipolar cell-photoreceptor connectivity in the zebrafish (*Danio rerio*) retina. *The Journal of Comparative Neurology*,ÿ, *520*, 3786–3802. https://doi.org/10.1002/cne.23168

Marc, R. E., & Cameron, D. (2001) A molecular phenotype atlas of the retina zebrafish. *Journal of Neurocytology*, *30*, 593–654. https://doi.org/10.1023/a:1016516818393

Mathieu, M., Tagliafierro, G., Bruzzone, F., & Vallarino, M. (2002). Neuropeptide tyrosine-like immunoreactive system in the brain, olfactory organ and retina of the zebrafish, *Danio rerio*, during development. *Developmental Brain Research*, *139*, 255–265. https://doi.org/10.1016/S0165-3806(02)00577-1

McCormick, C. A., & Hernández, D. V. (1996). Connections of octaval and lateral line nuclei of the medulla in the goldfish, including the cytoarchitecture of the secondary octaval population in goldfish and catfish. *Brain, Behavior and Evolution*, *47*, 113–137. https://doi.org/10.1159/000113232

Meek, J., & Nieuwenhuys, R. (1998). Holosteans and teleosts. In R. Nieuwenhuys, H. J. ten Donkelaar, & C. Nicholson (Eds.), *The central nervous system of vertebrates* (pp. 759–937). Springer.

Meek, J., & Schellart, N. A. M. (1978). A Golgi study of goldfish optic tectum. *The Journal of Comparative Neurology*, *182*, 89–122. https://doi.org/10.1002/cne.901820107

Meredith, G. E. (1984). Peripheral configuration and central projections of the lateral line system in *Astronotus ocellatus* (Cichlidae): A nonelectroreceptive teleost. *The Journal of Comparative Neurology*, *228*, 342–358. https://doi.org/10.1002/cne.902280305

Miyamura, Y., & Nakayasu, H. (2001). Zonal distribution of Purkinje cells in the zebrafish cerebellum: Analysis by means of a specific monoclonal antibody. *Cell and Tissue Research*, *305*, 299–305. https://doi.org/10.1007/s004410100421

Mueller, T., & Guo, S. (2009). The distribution of GAD67-mRNA in the adult zebrafish (teleost) forebrain reveals a prosomeric pattern and suggests previously unidentified homologies to tetrapods. *The Journal of Comparative Neurology*, *516*, 553–568. https://doi.org/10.1002/cne.22122

Mueller, T., Vernier, P., & Wullimann, M. F. (2004). The adult central nervous cholinergic system of a neurogenetic model animal, the zebrafish *Danio*

rerio. *Brain Research*, *1011*, 156–169. https://doi.org/10.1016/j.brainres.2004.02.073

Murakami, T., & Morita, Y. (1987). Morphology and distribution of the projection neurons in the cerebellum in a teleost, *Sebastiscus marmoratus*. *The Journal of Comparative Neurology*, *256*, 607–623. https://doi.org/10.1002/cne.902560413

Nevin, L. M., Taylor, M. R., & Baier, H. (2008). Hardwiring of fine synaptic layers in the zebrafish visual pathway. *Neural Development*, *3*(36). https://doi.org/10.1186/1749-8104-3-36

Nieuwenhuys, R. (1967). Comparative anatomy of the cerebellum. *Progress in Brain Research*, *25*, 1–93. https://doi.org/10.1016/S0079-6123(08)60962-0

Nieuwenhuys, R. (2009). The forebrain of actinopterygians revisited. *Brain, Behavior and Evolution*, *73*, 229–252. https://doi.org/10.1159/000225622

Northcutt, R. G. (1995). The forebrain of gnathostomes: In search of a morphotype. *Brain, Behavior and Evolution*, *46*, 275–318. https://doi.org/10.1159/000113279

Northcutt, R. G. (2008). Forebrain evolution in bony fishes. *Brain Research Bulletin*, *75*, 191–205. https://doi.org/10.1016/j.brainresbull.2007.10.058

Northcutt, R. G. (2011). Olfactory projections in the white sturgeon, *Acipenser transmontanus*: An experimental study. *The Journal of Comparative Neurology*, *519*, 1999–2022. https://doi.org/10.1002/cne.22619

Pak, J. H., Huang, F. L., Li, J., Balschun, D., Reymann, K. G., Chiang, C., Westphal, H., & Huang, K. P. (2000) Involvement of neurogranin in the modulation of calcium/calmodulin-dependent protein kinase II, synaptic plasticity, and spatial learning: A study with knockout mice. *Proceedings of the National Academy of Science of the United States of America*, *97*, 11232–11237. https://doi.org/10.1073/pnas.210184697

Piosik, P. A., Van Groenigen, M., Ponne, N. J., Bolhuis, P. A., & Baas, F. (1995). RC3/neurogranin structure and expression in the caprine brain in relation to congenital hypothyroidism. *Molecular Brain Research*, *29*, 119–130. https://doi.org/10.1016/0169-328X(94)00237-9

Portavella, M., Vargas, J. P., Torres, B., & Salas, C. (2002). The effects of telencephalic pallial lesions on spatial, temporal, and emotional learning in goldfish. *Brain Research Bulletin*, *57*, 397–399. https://doi.org/10.1016/s0361-9230(01)00699-2

Portavella, M., Torres, B., & Salas, C. (2004). Avoidance response in goldfish: Emotional and temporal involvement of medial and lateral telencephalic pallium. *The Journal of Neuroscience*, *24*, 2335–2342. https://doi.org/10.1523/jneurosci.4930-03.2004

Porter, B. A., & Mueller, T. (2020). The zebrafish amygdaloid complex - Functional ground plan, molecular delineation, and everted topology. *Frontiers Neuroscience*, *14*, 608. https://doi.org/10.3389/fnins.2020.00608 PMID: 32765204; PMCID: PMC7378821.

Prichard, L., Deloulme, J. C., & Storm, D. R. (1999). Interactions between neurogranin and calmodulin in vivo. *The Journal of Biological Chemistry*, *274*, 7689–7694. https://doi.org/10.1074/jbc.274.12.7689

Represa, A., Deloulme, J. C., Sensenbrenner, M., Ben-Ari, Y., & Baudier, J. (1990). Neurogranin: Immunocytochemical localization of a brain-specific protein kinase C substrate. *The Journal of Neuroscience*, *10*, 3782–3792. https://doi.org/10.1523/jneurosci.10-12-03782.1990

Rink, E., & Wullimann, M. F. (2004). Connections of the ventral telencephalon (subpallium) in the zebrafish (*Danio rerio*). *Brain Research*, *1011*, 206–220. https://doi.org/10.1016/j.brainres.2004.03.027

Robinson, J., Schmitt, E. A., Harosit, F. I., Reecet, R. J., & Dowling, J. E. (1993). Zebrafish ultraviolet visual pigment: Absorption spectrum, sequence, and localization. *Proceedings of the National Academy of Science of the United States of America*, *90*, 6009–6012. https://doi.org/10.1073/pnas.90.13.6009

Saidel, W. M. (2013). Nucleus rostrolateralis: An expansion of the epithalamus in some actinopterygii. *Anatomical Record*, *296*, 1594–1602. https://doi.org/10.1002/ar.22761

Saidel, W. M., & Butler, A. B. (1997). An atypical diencephalic nucleus in actinopterygian fishes: Visual connections and sporadic phylogenetic distribution. *Neuroscience Letters*, *229*, 13–16. https://doi.org/10.1016/S0304-3940(97)00411-4

Salbreux, G., Barthel, L. K., Raymond, P. A., & Lubensky, D. K. (2012). Coupling mechanical deformations and planar cell polarity to create regular patterns in the zebrafish retina. *PLoS Computational Biology*, *8*, 1–20. https://doi.org/10.1371/journal.pcbi.1002618

Schäffer, A. A., Aravind, L., Madden, T. L., Shavirin, S., Spouge, J. L., Wolf, Y. I., Koonin, E. V., & Altschul, S. F. (2001). Improving the accuracy of PSI-BLAST protein database searches with composition-based statistics and other refinements. *Nucleic Acids Research*, *29*, 2994–3005. https://doi.org/10.1093/nar/29.14.2994

Schmidt, R., Strähle, U., & Scholpp, S. (2013). Neurogenesis in zebrafish – from embryo to adult. *Neural Development*, *8*(3). https://doi.org/10.1186/1749-8104-8-3

Sherry, D. S., & Yazulla, S. (1993). Goldfish bipolar cells and axon terminal patterns: A Golgi study. *The Journal of Comparative Neurology*, *329*, 188–200. https://doi.org/10.1002/cne.903290204

Simat, M., Parpan, F., & Fritschy, J. M. (2007). Heterogeneity of glycinergic and gabaergic interneurons in the granule cell layer of mouse cerebellum. *The Journal of Comparative Neurology*, *500*, 71–83. https://doi.org/10.1002/cne.21142

Singec, I., Knoth, R., Ditter, M., Volk, B., & Frotscher, M. (2004). Neurogranin is expressed by principal cells but not interneurons in the rodent and monkey neocortex and hippocampus. *The Journal of Comparative Neurology*, *479*, 30–42. https://doi.org/10.1002/cne.20302

Slemmon, J. R., Morgan, J. I., Fullerton, S. M., Danho, W., Hilbush, B. S., & Wengenack, T. M. (1996). Camstatins are peptide antagonists of calmodulin based upon a conserved structural motif in PEP-19, neurogranin, and neuromodulin. *The Journal of Biological Chemistry*, *271*, 15911–15917. https://doi.org/10.1074/jbc.271.27.15911

Slemmon, J. R., Feng, B., & Erhardt, J. A. (2000). Small proteins that modulate calmodulin-dependent signal transduction: Effects of PEP-19, neuromodulin, and neurogranin on enzyme activation and cellular homeostasis. *Molecular Neurobiology*, *22*, 99–113. https://doi.org/10.1385/mn:22:1-3:099

Smeraski, C. A., Dunwiddie, T. V., Diao, L., & Finger, T. E. (1999). NMDA and non-NMDA receptors mediate NMDA and non-NMDA receptors mediate responses in the primary gustatory nucleus in goldfish. *Chemical Senses*, *24*, 37–46. https://doi.org/10.1093/chemse/24.1.37

Sullivan, J. M., Grant, C. A., Reker, A. N., Nahar, L., Goeders, N. E., & Nam, H. W. (2019). Neurogranin regulates sensorimotor gating through cortico-striatal circuitry. *Neuropharmacology*, *150*, 91–99. https://doi.org/10.1016/j.neuropharm.2019.03.021

Takechi, M., Hamaoka, T., & Kawamura, S. (2003). Fluorescence visualization of ultraviolet-sensitive cone photoreceptor development in living zebrafish. *Federation of European Biochemical Societies Letters*, *553*, 90–94. https://doi.org/10.1016/s0014-5793(03)00977-3

Tejero-Díez, P., Rodríguez-Sánchez, P., & Díez-Guerra, J. (1999). Microscale purification of proteins exhibiting anomalous electrophoretic migration: Application to the analysis of GAP-43 phosphorylation. *Analytical Biochemistry*, *274*, 278–282. https://doi.org/10.1006/abio.1999.4292

Turner, K. J., Hawkins, T. A., Yáñez, J., Anadón, R., Wilson, S. W., & Folgueira, M. (2016). Afferent connectivity of the zebrafish habenulae. *Frontiers in Neural Circuits*, *10*(30). https://doi.org/10.3389/fncir.2016.00030

Vanegas, H., Laufer, M., & Amat, J. (1974). The optic tectum of a perciform teleost I. General configuration and cytoarchitecture. *The Journal of Comparative Neurology*, *154*, 43–60. https://doi.org/10.1002/cne.901540104

Watson, J. B., Battenberg, E. F., Wong, K. K., Bloom, F. E., & Sutcliffe, J. G. (1990). Subtractive cDNA cloning of RC3, a rodent cortex-enriched mRNA encoding a novel 78 residue protein. *Journal of Neuroscience Research*, *26*, 397–408. https://doi.org/10.1002/jnr.490260402

Watson, J. B., Margulies, J. E., Coulter, P. M., Gerendasy, D. D., Sutcliffe, J. G., & Cohen, R. W. (1996). Functional studies of single-site

variants in the calmodulin-binding domain of RC3/neurogranin in Xenopus oocytes. *Neuroscience Letters*, *219*, 183–186. https://doi.org/10.1016/s0304-3940(96)13203-1

Watson, J. B., Sutcliffet, J. G., & Fishert, R. S. (1992). Localization of the protein kinase C phosphorylation/calmodulin-binding substrate RC3 in dendritic spines of neostriatal neurons. *Proceedings of the National Academy of Sciences of the United States of America*, *89*, 8581–8585. https://doi.org/10.1073/pnas.89.18.8581

White, J. J., & Sillitoe, R. V. (2013). Postnatal development of cerebellar zones revealed by neurofilament heavy chain protein expression. *Frontiers in Neuroanatomy*, *9*, 7. https://doi.org/10.3389/fnana.2013.00009

Wong, K. S., Proulx, K., Rost, M. S., & Sumanas, S. (2009). Identification of vasculature-specific genes by microarray analysis of Etsrp/Etv2 overexpressing zebrafish embryos. *Developmental Dynamics*, *238*, 1836–1850. https://doi.org/10.1002/dvdy.21990

Wu, J., Huang, K. P., & Huang, F. L. (2003). Participation of NMDA-mediated phosphorylation and oxidation of neurogranin in the regulation of Ca^{2+} and Ca^{2+}/calmodulin-dependent neuronal signaling in the hippocampus. *Journal of Neurochemistry*, *86*, 1524–1533. https://doi.org/10.1046/j.1471-4159.2003.01963.x

Wullimann, M. F., & Mueller, T. (2004). Teleostean and mammalian forebrains contrasted: Evidence from genes to behavior. *The Journal of Comparative Neurology*, *475*, 143–162. https://doi.org/10.1002/cne.20183

Wullimann, M. F., Rupp, B., & Reichert, H. (1996). A topological atlas. In M.F. Wullimann, B. Rupp, & H. Reicher (Eds.), *Neuroanatomy of the zebrafish brain* (pp. 1–84). Birkhäuser.

Xavier, A. L., Fontaine, R., Bloch, S., Affaticati, P., Jenett, A., Demarque, M., Vernier, P., & Yamamoto, K. (2017). Comparative analysis of monoaminergic cerebrospinal fluid-contacting cells in *Osteichthyes* (bony vertebrates). *The Journal of Comparative Neurology*, *525*, 2265–2283. https://doi.org/10.1002/cne.24204

Xiang, Y., Xin, J., Le, W., & Yang, Y. (2020). Neurogranin: A potential biomarker of neurological and mental diseases. *Frontiers in Aging Neuroscience*, *12*(584743). https://doi.org/10.3389/fnagi.2020.584743

Yamamoto, K., Ruuskanen, J. O., Wullimann, M. F., & Vernier, P. (2010). Two tyrosine hydroxylase genes in vertebrates: New dopaminergic territories revealed in the zebrafish brain. *Molecular and Cell Neuroscience*, *43*(4), 394–402. https://doi.org/10.1016/j.mcn.2010.01.006

Yamamoto, K., Ruuskanen, J. O., Wullimann, M. F., & Vernier, P. (2011). Differential expression of dopaminergic cell markers in the adult zebrafish forebrain. *The Journal of Comparative Neurology*, *519*, 576–598. https://doi.org/10.1002/cne.22535

Yamamoto, K., Bloch, S., & Vernier, P. (2017). New perspective on the regionalization of the anterior forebrain in *Osteichthyes*. *Development, Growth and Differentiation*, *59*, 175–187. https://doi.org/10.1111/dgd.12348

Yamamoto, N., Ishikawa, Y., Yoshimoto, M., Xue, H., Bahaxar, N., Sawai, N., Yang, C., Ozawa, H., & Ito, H. (2007). A new interpretation on the homology of the teleostean telencephalon based on hodology and new eversion model. *Brain, Behavior and Evolution*, *69*, 96–104. https://doi.org/10.1159/000095198

Yamamoto, N., Kato, T., Okada, Y., & Somiya, H. (2010). Somatosensory nucleus in the torus semicircularis of cyprinid teleosts. *The Journal of Comparative Neurology*, *518*, 2472–2502. https://doi.org/10.1002/cne.22348

Yang, C. Y., Yoshimoto, M., Xue, H. G., Yamamoto, N., Imura, K., Sawai, N., Ishikawa, Y., & Ito, H. (2004). Fiber connections of the lateral valvular nucleus in a percomorph teleost, tilapia (*Oreochromis niloticus*). *The Journal of Comparative Neurology*, *474*, 209–226. https://doi.org/10.1002/cne.20150

Yáñez, J., Folgueira, M., Lamas, I., & Anadón, R. (2021). The organization of the zebrafish pallium from a hodological perspective. *The Journal of Comparative Neurology*. Advance online publication. https://doi.org/10.1002/cne.25268.

Yang, J., Korley, F. K., Dai, M., & Everett, A. D. (2015). Serum neurogranin measurement as a biomarker of acute traumatic brain injury. *Clinical Biochemistry*, *48*, 843–848. https://doi.org/10.1016/j.clinbiochem.2015.05.015

Yáñez, J., Souto, Y., Piñeiro, L., Folgueira, M., & Anadón, R. (2017). Gustatory and general visceral centers and their connections in the brain of adult zebrafish: A carbocyanine dye tract-tracing study. *The Journal of Comparative Neurology*, *525*, 333–362. https://doi.org/10.1002/cne.24068

Yáñez, J., Suárez, T., Quelle, A., Folgueira, M., & Anadón, R. (2018). Neural connections of the pretectum in zebrafish (*Danio rerio*). *The Journal of Comparative Neurology*, *526*, 1017–1040. https://doi.org/10.1002/cne.24388

Yazulla, S., & Studholme, K. (2001). Neurochemical anatomy of the zebrafish retina as determined by immunocytochemistry. *Journal of Neurocytology*, *30*, 551–592. https://doi.org/10.1023/a:1016512617484

Zada, D., Tovin, A., Lerer-Goldshtein, T., Vatine, G. D., & Appelbaum, L. (2014). Altered behavioral performance and live imaging of circuit-specific neural deficiencies in a zebrafish model for psychomotor retardation. *PLoS Genetics*, *10*(9). https://doi.org/10.1371/journal.pgen.1004615

Zhong, L., Cherry, T., Bies, C. E., Florence, M. A., & Gerges, N. Z. (2009). Neurogranin enhances synaptic strength through its interaction with calmodulin. *EMBO Journal*, *28*, 3027–3039. https://doi.org/10.1038/emboj.2009.236

Zhong, L., Brown, J., Kramer, A., Kaleka, K., Petersen, A., Krueger, J. N., Florence, M., Muelbl, M. J., Battle, M., Murphy, G. G., Olsen, C. M., & Gerges, N. Z. (2015). Increased prefrontal cortex neurogranin enhances plasticity and extinction learning. *Journal of Neuroscience*, *35*, 7503-7508. https://doi.org/10.1523/jneurosci.0274-15.2015

Zhong, L., & Gerges, N. Z. (2012). Neurogranin targets calmodulin and lowers the threshold for the induction of long-term potentiation. *PloS One*, *7*(7), e41275. https://doi.org/10.1371/journal.pone.0041275

Zhong, L., & Gerges, N. Z. (2020). Neurogranin regulates metaplasticity. *Frontiers in Molecular Neuroscience*, *12*, 322. https://doi.org/10.3389/fnmol.2019.00322

Zhong, L., Kaleka, K. S., & Gerges, N. Z. (2011). Neurogranin phosphorylation fine-tunes long-term potentiation. *European Journal of Neuroscience*, *33*, 244–250. https://doi.org/10.1111/j.1460-9568.2010.07506.x

How to cite this article: Alba-González, A., Folgueira, M., Castro, A., Anadón, R., & Yáñez, J. (2022). Distribution of neurogranin-like immunoreactivity in the brain and sensory organs of the adult zebrafish. *J Comp Neurol*. *530*, 1569–1587. https://doi.org/10.1002/cne.25297